Thebault, E., Vervelidou, F. (2015): A statistical spatial power spectrum of the Earth's lithospheric magnetic field. - *Geophysical Journal International*, *201*, 2, p. 605-620.

DOI: http://doi.org/10.1093/gji/ggu463

Geophysical Journal International

Geophys. J. Int. (2015) **201,** 605–620 doi: 10.1093/gji/ggu463

GJI Geomagnetism, rock magnetism and palaeomagnetism

A statistical spatial power spectrum of the Earth's lithospheric magnetic field

E. Thébault[1,*] and F. Vervelidou[2,*]

[1] *UMR CNRS* 6112, *University of Nantes, Laboratoire de Planétologie et de Géodynamique, UMR*-6112, 2 *rue de la Houssiniere, France. E-mail: erwan.thebault@univ-nantes.fr*

[2] *Helmholtz Centre Potsdam, GFZ German Research Centre for Geosciences, Telegrafenberg, D*-14473 *Potsdam, Germany*

Accepted 2014 December 2. Received 2014 November 25; in original form 2014 July 22

SUMMARY

The magnetic field of the Earth's lithosphere arises from rock magnetization contrasts that were shaped over geological times. The field can be described mathematically in spherical harmonics or with distributions of magnetization. We exploit this dual representation and assume that the lithospheric field is induced by spatially varying susceptibility values within a shell of constant thickness. By introducing a statistical assumption about the power spectrum of the susceptibility, we then derive a statistical expression for the spatial power spectrum of the crustal magnetic field for the spatial scales ranging from 60 to 2500 km. This expression depends on the mean induced magnetization, the thickness of the shell, and a power law exponent for the power spectrum of the susceptibility. We test the relevance of this form with a misfit analysis to the observational NGDC-720 lithospheric magnetic field model power spectrum. This allows us to estimate a mean global apparent induced magnetization value between 0.3 and 0.6 A m^{-1}, a mean magnetic crustal thickness value between 23 and 30 km, and a root mean square for the field value between 190 and 205 nT at 95 per cent. These estimates are in good agreement with independent models of the crustal magnetization and of the seismic crustal thickness. We carry out the same analysis in the continental and oceanic domains separately. We complement the misfit analyses with a Kolmogorov–Smirnov goodness-of-fit test and we conclude that the observed power spectrum can be each time a sample of the statistical one.

Key words: Electromagnetic theory; Magnetic anomalies: modelling and interpretation; Satellite magnetics.

1 INTRODUCTION

The magnetic field of the Earth results from complex dynamic processes in the core, the lithosphere and regions external to the Earth's surface (e.g. Hulot *et al.* 2007, for a review). The magnetic field of the Earth's lithosphere arises from rock magnetization contrasts that were shaped over geological times. This magnetic signal reflects the properties and the composition of the Earth's crust and represents an invaluable source of information to decipher its history. Since the epoch of the Magsat satellite (1979–1980), the lithospheric magnetic field at global scales has been represented in terms of spherical harmonics (SH). The SH mathematical representation indicates that the lithospheric magnetic field is masked by the main field for the spatial scales larger than about 2500 km (e.g. Langel & Estes 1982), and partially known for the spatial scales smaller than about 400 km as a result of overlapping contributions of other source fields and the incomplete availability of the magnetic measurements on a global scale (e.g. Purucker & Whaler 2007). In principle, a better description of the lithospheric magnetic field over a very wide range of spatial scales could be obtained by inferring rules about its nature. Such information would be useful to allow some recovery of its masked contributions. Studies focused on this long-standing question have, however, concluded that the interpretation of the crustal magnetic field is not univocal (unambiguous) because it results from many competing influences (e.g. Langel & Hinze 1998; chapter 7). The source magnetization may be remanent or induced (e.g. Counil *et al.* 1991; Dyment & Arkani-Hamed 1998; Maus & Haak 2002). Magnetization contrasts can be modified or caused by heat flow anomalies (e.g. Mayhew 1985; Fox-Maule *et al.* 2005; Bouligand *et al.* 2009). The net contrast can vary with local crustal thickening or thinning (e.g. Purucker *et al.* 2002). It typically varies with composition and it changes both with chemical alteration of the rock and the shape of geological units (e.g. Hemant & Maus 2005).

*Previously at: Equipe de Géomagnétisme, Institut de Physique du Globe de Paris, Sorbonne Paris Cité, Université Paris Diderot, UMR CNRS 7154, 1 rue Jussieu, F-75005 Paris, France.

Moreover, the crustal field itself reflects only part of the true rock magnetization (e.g. Gubbins *et al.* 2011) due to source distributions that give no external field (the magnetic annihilators that were exemplified by Runcorn 1975). The deterministic studies explain many of the magnetic field structures observed at the satellite altitudes but they rarely account accurately for all the observed features in space. In general, it is fair to say that these studies explain most of the major magnetic anomalies but correlate only fairly well with SH representations of the magnetic field measurements even for the low SH degrees (Purucker *et al.* 2002; Hemant & Maus 2005).

The interpretation of the magnetic field is complicated by an inherent non-uniqueness but one major conclusion that emerges from these works is that the large-scale lithospheric magnetic field structures are mostly dominated by the horizontal fluctuations of the magnetic crustal depth and/or by the lateral contrasts in the magnetization of the geological units. For this reason, some scientists have focused their work on these two properties and tackled the problem of separating their very similar effects by statistical methods. Various statistical forms for the spatial power spectrum expressed in SH have been devised relying on first order physical principles. Jackson (1990, 1994) proposes two statistical spectra based on the assumption that the crustal magnetization is spatially randomly distributed, that it lies within a thin shell, and that it is characterized by a typical lateral correlation length. He then uses these expressions to constrain the waveband where the core and the crustal fields overlap (Jackson 1996). These statistical spectra, realistic considering our understanding of the Earth's crust, compare modestly to those of the measured data (Jackson 1996; O'Brien *et al.* 1999). In an effort to better understand the origin of these discrepancies, Voorhies (1998) derives an ensemble of expressions for the spatial power spectrum based on random or aligned magnetization distributions located within thin, thick, spherical, or ellipsoidal shells. Among this variety of spectra, Voorhies *et al.* (2002) find a class that provides estimated values for the magnetic crustal thickness in general agreement with the fact that ferrimagnetic minerals, the principal source of crustal magnetic field, should not be massively present in the mantle (Wasilewski & Mayhew 1992). However, they also conclude that these physically motivated statistical forms show systematic and significant deviations from the measured power spectrum of the Earth's magnetic lithospheric field.

This paper continues these pioneering global studies, but with inspiration and guidance from theoretical works focused on the analysis and interpretation of regional scale magnetic observations. Pilkington & Todoeschuck (1993, 1995), for instance, show that the apparent susceptibility could be self-similar on regional scales. Maus & Dimri (1994) and Maus *et al.* (1997) elaborate on this idea to propose an expression for the plane magnetic power spectrum as a function of the mean magnetization, the crustal thickness, and a power law for the 3-D susceptibility distribution. Such an expression, which supersedes the more standard determination of the depth to the bottom (DTB) based on the assumption that the magnetic field should exhibit a flat power spectrum (e.g. Spector & Grant 1970), agree reasonably well with the observed planar power spectra. These concepts developed in the framework of exploration geophysics can be implemented at the global scale by assuming that the SH power spectrum of the susceptibility follows a power law.

We tackle the problem in SH in a pseudo-statistical way, midway between deterministic and statistical, and we first assume that the lithospheric magnetic field is induced in a spherical shell. We then summarize the key steps needed to derive an expression of the lithospheric magnetic field power spectrum in SH in terms of an equivalent susceptibility distribution. By making statistical assumptions on the power spectrum of the susceptibility, we deduce a new statistical form for the spatial power spectrum of the lithospheric magnetic field. We take advantage of the recent lithospheric field models (e.g. Thébault *et al.* 2010, for a review) to test and to assess the relevance of the parametrization. This permits us to estimate the mean thickness of the Earth's magnetic crust, its mean magnetization, and the mean value of the exponent of the susceptibility power spectrum and to compare them with values inferred from independent geophysical models. We illustrate the statistical properties of the lithospheric magnetic field power spectrum for spatial scales ranging from about 50 to 2500 km and we discuss its possible applications.

2 EXPRESSION OF THE MAGNETIC FIELD IN TERMS OF LATERAL SUSCEPTIBILITY VARIATIONS

The internal magnetic potential of the Earth's lithosphere observed at the position $\mathbf{r}$ above the Earth's reference surface can be represented in SH following the notation of Backus *et al.* (1996, pp. 141–142)

$$V_{\mathrm{SH}}(\mathbf{r}) = a \sum_{l,m} \left(\frac{a}{r}\right)^{l+1} \beta_l^m(\theta, \varphi) g_l^m, \tag{1}$$

with $a = 6371.2$ km the Earth's reference radius, r, θ, φ the geocentric coordinates, g_l^m the Gauss coefficients, and where the SH functions β_l^m are Schmidt normalized. Assuming that the lithospheric magnetic field is produced by a continuous distribution of magnetization located within a spherical shell Ω' of elementary volume $\mathrm{d}\Omega'$, the magnetic potential takes also the integral form (e.g. Blakely 1995, eq. 5.2)

$$V_d(\mathbf{r}) = \frac{\mu_0}{4\pi} \int_{\Omega'} \mathbf{M}(\mathbf{r}') \cdot \nabla' \left(\frac{1}{|\mathbf{r} - \mathbf{r}'|}\right) \mathrm{d}\Omega', \tag{2}$$

where μ_0 is the vacuum permeability, $\mathbf{M}(\mathbf{r}')$ the magnetization vector, $\nabla'(.)$ the gradient operator applied on $\mathbf{r}'$ and $\mathbf{r}$ the point of observation (with $|\mathbf{r}| > |\mathbf{r}'|$). The two formalisms (eqs 1 and 2) provide equal magnetic potential values in the spatial domain so that a relationship between the SH Gauss coefficients g_l^m and the distribution of magnetization can be calculated (e.g. Gubbins *et al.* 2011 their eq. 7)

$$g_l^m = \frac{\mu_0}{4\pi a^{l+2}} \int_{\Omega'} \mathbf{M}(\mathbf{r}') \cdot \nabla' \left[r'^l \beta_l^m(\theta', \varphi')\right] \mathrm{d}\Omega'. \tag{3}$$

At this stage, we introduce the simplifying assumption that the lithospheric magnetic field is mostly induced by the Earth's main magnetic field. This may be seen as a strong hypothesis because remanent magnetic fields are often considered to dominate in oceans and in large continental igneous provinces. This hypothesis, however, might be softer that thought if we consider the global statistical properties of the lithospheric magnetic field that are the focus of this paper. First, young remanent field structures, including those in the oceans, are mostly co-linear (parallel or antiparallel) to the ambient magnetic field in the absence of systematic rotation of the tectonic blocks. Secondly, it can be shown analytically that the variation in degree l between the expected power spectrum for field-aligned dipoles of random polarity and that for dipoles oriented along the main inducing field does not exceed 2.5 per cent from degree 12 to infinity (Voorhies 1998, eq. 25a). Both power spectra are therefore statistically hardly separable in practice. At last, we must keep in

mind that the lithospheric field models derived to high spatial resolution rely mostly on scalar total intensity anomaly data that do not allow recovering the true direction of the crustal field vector components. As a result, the available lithospheric magnetic field models can hardly constrain more realistic and complex distributions of the Earth's lithospheric magnetic sources. For the sake of simplicity, we further assume that the inducing field is axial dipolar so that the magnetization vector writes

$$\mathbf{M}(\mathbf{r}') = \frac{\kappa(r',\varphi',\theta')}{\mu_0} g_1^0 \left(\frac{a}{r'}\right)^3 \left\{2\cos\theta' \mathbf{u}_r + \sin\theta' \mathbf{u}_\theta\right\}, \tag{4}$$

with $\kappa(r',\varphi',\theta')$ the apparent magnetic susceptibility that is also written as $\kappa(r',\varphi',\theta') = f(r')\widetilde{\kappa}(\varphi',\theta')$ and $(\mathbf{u}_r, \mathbf{u}_\theta)$ the unit vectors on the sphere, respectively radially upward and southward. From here, we follow the method detailed by Arkani-Hamed & Strangway (1985). The SH form an orthogonal basis so that we can expand $\widetilde{\kappa}(\varphi',\theta')$ in terms of β_l^m with the coefficients χ_l^m

$$\kappa(\mathbf{r}') = \sum_{l,m} f(r')\beta_l^m(\theta',\varphi')\chi_l^m. \tag{5}$$

We further make use of the SH recurrence formulas (in particular the formula 3.7.28 of Backus *et al.* 1996, p. 111) to obtain the relation between the lithospheric field Gauss coefficients g_l^m and the apparent susceptibility coefficients χ_l^m. We consider that the distribution of the magnetization lies within a spherical shell bounded by radii $r' = a$ and $a - \varepsilon$. By assuming so, we omit the effects of the lateral variation of the crustal thickness and assume that the lateral variation of the magnetic susceptibility is the primary magnetization process. We also consider that the top of the magnetic layer is the Earth's mean radius and therefore neglect the effect of weakly magnetized covers. The expression given at the Earth's mean radius is (see also Arkani-Hamed & Strangway 1985, their eq. 14)

$$g_l^m = \frac{g_1^0}{a}\int_{a-\varepsilon}^{a} f(r')\left(\frac{r'}{a}\right)^{l-2} dr'\left[\alpha_{l+1}^m \chi_{l+1}^m + \delta_{l-1}^m \chi_{l-1}^m\right], \tag{6}$$

with

$$\alpha_{l+1}^m = \frac{3l\left[(l+1)^2 - m^2\right]^{1/2}}{(2l+1)(2l+3)}, \tag{7}$$

and

$$\delta_{l-1}^m = \frac{(l-1)(l^2-m^2)^{1/2}}{(2l+1)(2l-1)}. \tag{8}$$

We need to define a vertical susceptibility distribution for performing the radial integration in eq. (6). In the absence of *a priori* information, we set $f(r') = 1$ so that

$$F_l(\varepsilon) = \frac{1}{a}\int_{a-\varepsilon}^{a} f(r')\left(\frac{r'}{a}\right)^{l-2} \mathrm{d}r' = \frac{\left[1-(1-\varepsilon/a)^{l-1}\right]}{l-1}. \tag{9}$$

The power-law dependency on $(r'/a)^{l-2}$ in eq. (6) and in the left member of the eq. (9) reflects the stronger influence of near surface susceptibility values on the shorter lithospheric field wavelengths. This property is imposed by the assumption that the magnetization is induced by the main field within the entire crustal thickness. The effect of this assumption is therefore not equivalent to assuming a vertically homogeneous magnetization (e.g. Hemant & Maus 2005; Gubbins *et al.* 2011) because the induced magnetization varies radially. However, it treats the susceptibility as if independent of radius within a magnetic crust thickness ε that is unrealistic locally. We argue that including the effects of vertically variable crustal susceptibility is necessary only at very small horizontal scales, smaller than the thickness of the crust itself.

We tested this claim and conducted two first-order analyses (not shown) with different radial distributions between $r' = a$ and $r' = a - \varepsilon$. We first put more weight near the surface than at depth to simulate decreasing magnetization caused by an increase of temperature with depth. Then, we assumed that the magnetization was mostly carried by the lower continental crust (e.g. Wasilewski & Mayhew 1982) and we considered a distribution with more weight at depth. These attempts unnecessarily complicate the theoretical form of our expressions and give similar numerical results. Therefore, we do not report further on these experiments. We refer to the work of Masterton (2010), where other numerical calculations are performed and described in details, and we conclude with this author (and others, see Langel & Hinze 1998, chapter 7) that the vertical distribution of the sources does not contribute significantly to the large-scale lithospheric magnetic field variations. In the present work, we shall therefore consider only the SH degrees 16–650 of lithospheric field models because they correspond to spatial scales large enough to neglect the vertical distribution of the susceptibility.

The eq. (9) is singular in $l = 1$ but converges to

$$\lim_{l\to 1} \frac{\left[1-(1-\varepsilon/a)^{l-1}\right]}{l-1} = -\ln(1-\varepsilon/a),$$

so that $F_l(\varepsilon)$ is defined for any SH degree l. The final expression relating the magnetic field to the susceptibility coefficients is

$$g_l^m = g_1^0 F_l(\varepsilon)\left[\alpha_{l+1}^m \chi_{l+1}^m + \delta_{l-1}^m \chi_{l-1}^m\right]. \tag{10}$$

This expression is valid to any arbitrary degree l provided our underlying assumptions are correct.

3 STATISTICS OF THE LITHOSPHERIC FIELD POWER SPECTRUM

The eq. (3), or the eq. (10) considering the sequence of hypotheses made so far, relates the crustal field gauss coefficients g_l^m to the apparent susceptibility coefficients χ_l^m. It could in principle be used to predict the values of the g_l^m Gauss coefficients in a deterministic way. This could be achieved using a model for the apparent susceptibility of the Earth's crust such as the one proposed by Hemant & Maus (2005) built on seismic, geological and tectonic maps of the world, laboratory susceptibility values of the rock types, and a magnetization model for the ocean floors. These types of models, however, are also imperfect and do neither exactly describe the geographical variations of the apparent susceptibility nor do they predict correctly the lithospheric magnetic field power spectrum (for instance Thébault *et al.* 2009, their fig. 1). Moreover, the series of assumptions made to derive the eq. (10) are too simplistic to explain reasonably well the geographical variations in the geomagnetic lithospheric field. The deterministic calculation of the g_l^m coefficients from a set of susceptibility coefficients χ_l^m is therefore not yet tractable and we propose to infer simpler and more general statistical rules characterizing the lithospheric magnetic field or its sources.

The total power of the magnetic potential in eq. (1) defined on the sphere is related to the sum of square of its spectral coefficients g_l^m. In practice, we do not measure the potential but the magnetic field and the total energy of the magnetic field in SH averaged over the reference sphere can be separated into its individual contribution for each degree l. Following Lowes (1966, 1974), the so-called spatial

power spectrum of the vector geomagnetic field at the Earth's mean radius is defined for each degree l as the element

$$R_l = (l+1)\sum_{m=-l}^{l}\left(g_l^m\right)^2. \tag{11}$$

The distribution of R_l in l is also often called the degree variance. A common strategy to bypass the absence of exact knowledge on the coefficients g_l^m is to rely on some statistical characterization and to test whether the observations could be a sample of the chosen statistical process. Let us consider that the lithospheric field degree variance R_l is a random variable whose expected value is

$$E\left\{R_l\right\} = (l+1)\sum_{m=-l}^{l} E\left\{\left(g_l^m\right)^2\right\}, \tag{12}$$

with according to eq. (10)

$$\begin{aligned} E\left\{\left(g_l^m\right)^2\right\} &= \left[g_1^0 F_l(\varepsilon)\right]^2 E\left\{\left(\alpha_{l+1}^m \chi_{l+1}^m + \delta_{l-1}^m \chi_{l-1}^m\right)^2\right\}, \\ &= \left[g_1^0 F_l(\varepsilon)\right]^2 \left[\left(\alpha_{l+1}^m\right)^2 E\left\{\left(\chi_{l+1}^m\right)^2\right\} + \left(\delta_{l-1}^m\right)^2 E\left\{\left(\chi_{l-1}^m\right)^2\right\}\right. \\ &\quad \left. + 2\alpha_{l+1}^m \delta_{l-1}^m E\left\{\chi_{l+1}^m \chi_{l-1}^m\right\}\right]. \end{aligned} \tag{13}$$

The function of the crustal thickness $F_l(\varepsilon)$ is given in eq. (9) and the parameters α_{l+1}^m and δ_{l-1}^m are defined in eqs (7) and (8). The form (13) shows that looking for *a priori* statistical information on the Gauss coefficients g_l^m requires us to specify the statistics on the coefficients χ_l^m and their correlation. Such statistical hypotheses can be defined for the susceptibility $\kappa(r)$ in the spatial domain. This is a line traditionally followed in geomagnetism, where processes involving spatially uncorrelated or slightly correlated sources have been often considered (for instance Jackson 1990, 1994; Voorhies 1998). One major difficulty with this approach is to define *a priori* a realistic correlation function for the sources when our knowledge of the source magnetization is incomplete and in general indirect. Here, we work in the SH spectral domain and we more conveniently make an assumption directly on the covariance of the susceptibility coefficients $E\{\chi_l^m \chi_{l'}^{m'}\}$ without making an explicit assumption on the susceptibility $\kappa(r)$ in space. For this, we exploit suggestions made by some authors that the magnetization distributions in space could be self-similar on local scales (e.g. Pilkington & Todoeschuck 1993) or could have scaling laws as a result of complex non-linear dynamic processes shaping the Earth's crust (Lovejoy *et al.* 2001). We recall that the degree variance of a scalar quantity in SH on a unitary sphere writes

$$E\left\{S_l\right\} = \frac{1}{4\pi}\sum_{m=-l}^{l} E\left\{\left(\chi_l^m\right)^2\right\}\left\|\beta_l^m(\theta,\varphi)\right\|^2,$$

so that

$$E\left\{S_l\right\} = \frac{1}{2l+1}\sum_{m=-l}^{l} E\left\{\left(\chi_l^m\right)^2\right\},$$

for a quasi Schmidt normalization of the functions β_l^m. Noting further that self-similar processes have the property to exhibit power law spectra, we impose

$$E\left\{S_l\right\} = \sigma_\chi^2 l^{-\gamma}, \tag{14}$$

which follows a power law and shows a constant slope equal to $-\gamma$ in a log–log scale. We stress that assuming that the susceptibility power spectrum follows a power law is an hypothesis less restrictive than assuming that the susceptibility is self-similar in the spatial domain. The two processes, however, share this property in the spectral domain. In general, the eq. (14) is not much informative about the sources in space and a large class of spatial susceptibility distributions could lead to the same spectral form. Among all possibilities, we note that the eq. (14) could be obtained by assuming that the set of coefficients $\{\chi_l^m\}$ are independent Gaussian variables with zero mean and variance $\sigma_\chi^2 l^{-\gamma}$ and that the susceptibility coefficients could be uncorrelated so that

$$E\left\{\chi_l^m \chi_{l'}^{m'}\right\} = \sigma_l^2 \delta_{ll'}\delta_{mm'} = \sigma_\chi^2 l^{-\gamma}\delta_{ll'}\delta_{mm'}, \tag{15}$$

where δ_{ij} is the Kronecker symbol (not to be confused with the parameter δ_{l-1}^m defined in eq. 8), l the SH degree, and σ_χ^2 a constant. For this statistical process, the set of susceptibility coefficients have a constant variance per degree l so that the susceptibility statistical model in space is invariant under rotation on the sphere. This seems is a natural and reasonable assumption regarding the distribution of the magnetic sources on Earth that have *a priori* no preferred reference frame. Since uncorrelated sources in space produce a rising susceptibility power spectrum, the form of eq. (12), as described with the eq. (14) and assuming (15), also implies that the susceptibility must be correlated in space for this process. For uncorrelated spatial sources, the susceptibility power spectrum must rise in l and the one of the crustal field in l^3 (see for instance Hulot and Le Mouel 1994 their section 2; Jackson 1994; or Voorhies 1998, and his section 2.2). This opens the possibility of estimating a typical correlation length for the sources and subsequently for the crustal field (e.g. Rygaard-Hjalsted *et al.* 1997, their eqs 7 and 19, respectively). These interesting questions related to the characterization of the statistical susceptibility distribution in space and its implication for the lithospheric field model are outside the scope of the present study although we propose some elements of discussion in the Appendix.

According to the eqs (13) and (15) the sum over the orders m in eq. (12) writes

$$\begin{aligned} \sum_{m=-l}^{l} E\left\{\left(g_l^m\right)^2\right\} &= \left(g_1^0 F_l(\varepsilon)\right)^2 \sum_{m=-l}^{l}\left[\left(\alpha_{l+1}^m\right)^2 E\left\{\left(\chi_{l+1}^m\right)^2\right\}\right. \\ &\quad \left. + \left(\delta_{l-1}^m\right)^2 E\left\{\left(\chi_{l-1}^m\right)^2\right\}\right], \end{aligned} \tag{16}$$

with

$$E\left\{\left(\chi_{l+1}^m\right)^2\right\} = \sigma_\chi^2 (l+1)^{-\gamma}, \tag{17a}$$

$$E\left\{\left(\chi_{l-1}^m\right)^2\right\} = \sigma_\chi^2 (l-1)^{-\gamma}. \tag{17b}$$

It can be shown that the sums write, respectively,

$$\sum_{m=-l}^{l}\left(\alpha_{l+1}^m\right)^2 E\left\{\left(\chi_{l+1}^m\right)^2\right\} = \sigma_\chi^2 (l+1)^{-\gamma} C_{l+1}, \tag{18}$$

$$\sum_{m=-l}^{l}\left(\delta_{l-1}^m\right)^2 E\left\{\left(\chi_{l-1}^m\right)^2\right\} = \sigma_\chi^2 (l-1)^{-\gamma} C_{l-1}, \tag{19}$$

with

$$C_{l+1} = \frac{3l^2(l+1)}{(2l+3)(2l+1)}, \tag{20}$$

$$C_{l-1} = \frac{l(l-1)^2}{3(2l+1)(2l-1)}. \tag{21}$$

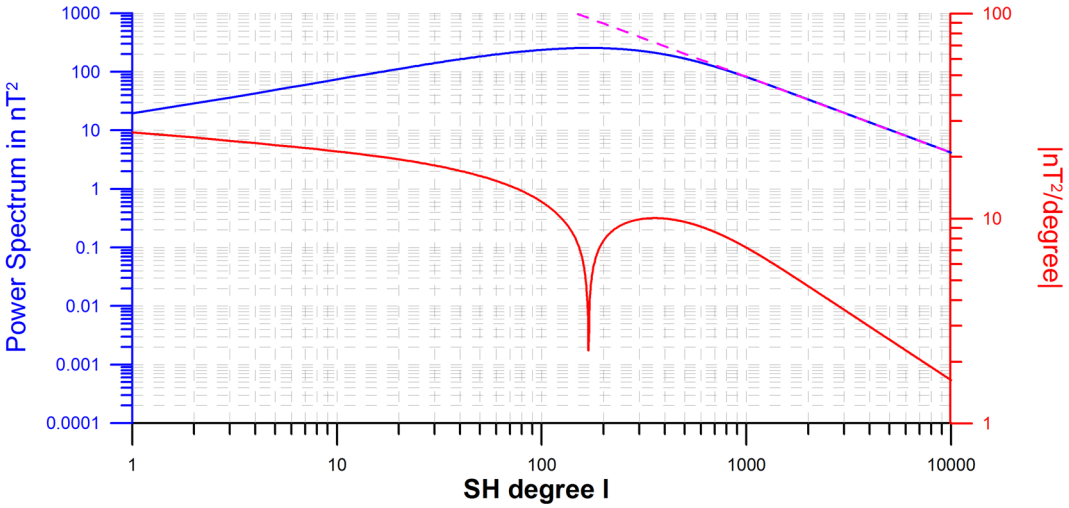

Figure 1. The statistical spherical power spectrum (blue curve) defined in eq. (26) is computed for $M = 0.7$ A m^{-1}, $\epsilon = 21$ km and $\gamma = 1.3$ for illustration purposes. The absolute value of its partial derivative in l is also sketched for a better indication of the power spectrum maximum that is reached near the SH degree 190. The dotted line (magenta) indicates that the slope can be assumed quasi-constant in a log–log scale from the SH degree about 1000.

The exact form under these statistical hypotheses is therefore

$$E\{R_l\} = (l+1)\left(g_1^0 F_l(\varepsilon)\sigma_\chi\right)^2 \left\{(l+1)^{-\gamma} C_{l+1} + (l-1)^{-\gamma} C_{l-1}\right\}. \tag{22}$$

Because we are mostly interested in the observed part of the lithospheric field at the SH degrees l larger than about 16, we may approximate $(l+1)$ and $(l-1)$ by l in the eqs (17a) and (17b) so that the expression (22) is approximately equal to

$$E\{R_l\} \simeq (l+1)\left(g_1^0 F_l(\varepsilon)\sigma_\chi\right)^2 l^{-\gamma} C_l, \tag{23}$$

with

$$C_l = \sum_{m=-l}^{l} \left[\left(\alpha_{l+1}^m\right)^2 + \left(\delta_{l-1}^m\right)^2\right] \tag{24}$$

$$= \frac{l(20l^3 + 8l^2 - 13l + 3)}{3(2l+3)(2l+1)(2l-1)}. \tag{25}$$

The relative difference between the eqs (22) and (23) decreases with the degree l. It does not exceed 6 per cent for the SH degrees above 16. Assuming $\mathfrak{m} = \sigma_\chi \langle F\rangle/\mu_0$ with $\langle F\rangle = \sqrt{2} g_1^0$ the magnetic field intensity of the axial dipole averaged over the sphere and $\mathfrak{m}$ the mean apparent induced magnetization, the equation (23) can finally be written

$$E\{R_l\} \simeq \frac{1}{2}(l+1)\left[\mu_0 \mathfrak{m} F_l(\varepsilon)\right]^2 l^{-\gamma} C_l, \tag{26}$$

where $F_l(\varepsilon)$ is given by the eq. (9) and C_l by eq. (25). The statistical degree variance of the lithospheric field $E\{R_l\}$ is in Tesla^2.

4 THE EXPECTED SPECTRUM OF THE LITHOSPHERIC FIELD

The Fig. 1 shows the expected power spectrum (eq. 26) in a log–log scale computed for $\mathfrak{m} = 0.7$ A m^{-1}, $\varepsilon = 21$ km, and $\gamma = 1.3$ (these values are chosen arbitrarily for discussion purposes). We also display the absolute value of its derivative in l ($|\partial_l E\{R_l\}|$) in order to highlight the location of the maximum. This statistical form has interesting properties and can be decomposed into two regions.

The first region defined for the low SH degrees is dominated by the effect of the equivalent thickness of the magnetic crust that gives this bell shape to the spectrum. The definitions of the geomagnetic power spectrum computed from global and regional data sets are not compatible and in general Fourier power spectra are computed from scalar anomaly intensity measurements. However, Maus (2008) proposes formulae to convert the power spectrum of regional aeromagnetic or marine surveys into SH and other authors (e.g. Beggan *et al.* 2013) have applied local expressions of power spectra on the sphere in terms of SH so that these formalisms could be readily compared to the statistical power spectrum given by the eq. (26). If we assume that the statistical process we described is stationary, the analysis of the theoretical form of the degree variance in SH sheds some interesting light on the expected regional variability of the SH magnetic field power spectrum.

In Fig. 1, we remark that the peak spreads over several hundreds of degrees l (between about $l = 100$ and 300 the spectrum has a comparable energy) and can only be identified by an accurate and broad-band view of the spectrum from the small to the large spatial scales. In order to identify the maximum of a power spectrum, one would need first to detect the increasing part that occurs at low SH degrees (or large wavelengths). If we extrapolate this result to a hypothetical regional survey, it means that a maximum in the power spectrum could hardly be identified clearly unless the survey has lateral extensions of several hundreds to thousands of kilometres (see also Maus *et al.* 1997 for a similar conclusion based on other arguments). In Fig. 2, we keep the same values for the magnetization and the γ exponent but we let the crustal thickness vary. We observe a shift of the maximum towards larger wavelengths for larger thicknesses. We see that the thickness of the continental crust, generally thought to be equal to values ranging from 20 to 80 km, produces a SH power spectrum maximum between the SH degrees 50 and 200. This corresponds to spatial scales that are in general poorly constrained by local surveys. On regional scales, it would therefore be often difficult to identify the maximum in power spectra, particularly in regions where the magnetic crust is thick.

Reversing this argument, we should therefore observe more easily maxima that occur at large wavenumbers in local power spectra when the magnetic crust is thin. In oceans, for instance, a mean thickness of 5 km should produce a maximum around the SH 830

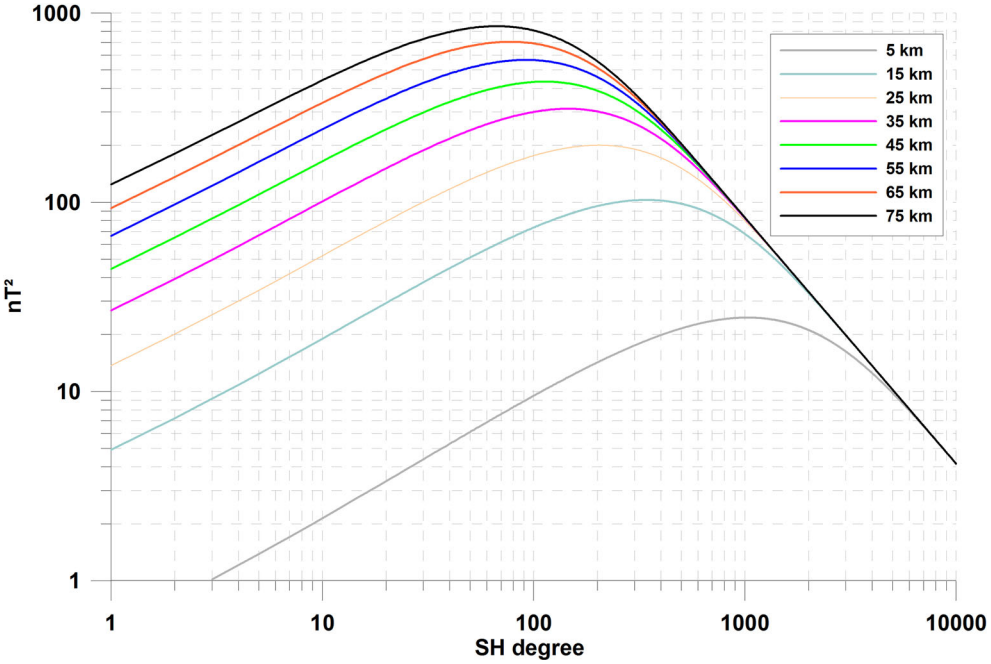

Figure 2. The statistical power spectrum defined by the eq. (26) is computed for SH degrees 1–10 000 with the parameters $\mathfrak{m} = 0.7$ A m^{-1}, the power-law exponent $\gamma = 1.3$ and crustal thickness values ε varying from 5 to 75 km. See text for a discussion.

(see Fig. 2). This spatial scale would be in principle detectable by regional magnetic surveys of sufficiently large geographical extension. The Fig. 2 shows that a difficulty arises because for 5 km thickness, the maximum difference between the power at the SH degrees 400 and 2000 does not exceed 5 nT^2. A regional spectrum computed from vector data acquired over a region of about 100 km of lateral extension would then appear nearly flat. This also conveys the important information that the depth to the bottom of the magnetic sources is intrinsically difficult to estimate accurately by methods relying on the analysis of the magnetic power spectrum.

Let us finally comment on the general decrease of the SH power spectrum that characterizes the second region. The statistical expression shows that the magnetic spectrum theoretically never follows a power law. However, after reaching a maximum, the spectrum decreases and asymptotically follows a regime where a constant slope in a log–log scale could be apparent. For $l \gg 1$, we have $F_l(\varepsilon) \propto l^{-1}$ (eq. 9) and $C_l \propto l$ (eq. 25) so that $E\{R_l\} \propto l^{-\gamma}$ (eq. 26) which shows that a power law for the magnetic spectrum is indeed asymptotically equal to the power law of the susceptibility degree variance (see eq. 14). In Fig. 1 (the magenta curve), this regime is reached (for the parameters considered in the calculation of this curve) around the SH degree 1000. As it is also illustrated in the Fig. 2, one difficulty is that this regime is reached asymptotically at varying SH degrees depending on the magnetic crustal thickness of the region under consideration. If we extrapolate this result to, again, a hypothetical regional survey, we are bound to conclude that regional variability in crustal thickness can introduce significant differences and uncertainties in the estimation of power laws unless we have models derived to very high SH degrees. We stress that our considerations are based on a theoretical expression of the spectrum in SH for which we made the approximation of a 2-D susceptibility distribution and omitted the oblateness of the Earth. For small spatial scales the effect of the vertical distribution of sources, their depth variation, and their distance to the Earth's mean radius may play a role that is not taken into account here (see Maus *et al.* 1997 for a 3-D planar expression).

Given these limitations, the statistical power spectrum we propose has two distinct regimes. The first one at low to intermediary SH degrees is shaped by the limited thickness of the magnetized layer. The second one appears at large SH degrees (wavelengths shorter than 50 km) and falls off to reach asymptotically a constant slope in log–log scale that characterizes the power law of the spectrum of the susceptibility.

5 SQUARE MISFIT TO A LOG OBSERVATIONAL SPECTRUM

We now test the relevance of the statistical expression (26) and its compatibility with the observations. During the last 60 yr, international groups of scientists put considerable efforts in mapping magnetic anomalies from local to regional scales making use of marine, aeromagnetic and satellite surveys (see Maus *et al.* 2009 and references therein). Recent progresses towards merging these heterogeneous data sets (Hamoudi *et al.* 2007; Hemant *et al.* 2007; Maus *et al.* 2007) in the framework of the project for the World Digital Magnetic Anomaly Map (Korhonen *et al.* 2007) have permitted the development of models depicting the Earth's crustal magnetic field over a wide range of SH degrees. The latest version of the NGDC-720 model (Maus 2010), for instance, is built upon the EMAG2 grid (Maus *et al.* 2009). It is a hybrid construction that uses the MF6 lithospheric magnetic field model (Maus *et al.* 2008) derived from the CHAMP satellite (Reigber & Lühr 2002) measurements for the SH degrees 16 to about 120, a world compilation of near-surface measurements for the higher SH degrees up to 720, and *prior* information about the preferred directions of the magnetic anomalies. The model takes a correction for the ellipsoid into account in order to avoid the distortions due to the spherical Earth's approximation that occur from the SH degree exceeding the real Earth reciprocal flattening (about $l = 300$ according to Voorhies 1998 in his section 4.1).

We do not restate the earlier comparisons made between lithospheric field model power spectra and the statistical forms published in the past as they are discussed elsewhere (see for example the fig. 1 of O'Brien *et al.* 1999; Voorhies *et al.* 2002; Vervelidou 2013). However we confirm that they fail in representing the NGDC-720 power spectrum over a large range of SH degrees and that they often indicate excessive source depth estimates (for instance Voorhies 1998 his section 7.4).

We fit the NGDC-720 degree variance R_l up to the SH degree 720, computed with the eq. (11), to $E\{R_l\}$, the statistical one whose expression is given by the eq. (26). We estimate the three unknown free parameters which are the power law exponent γ, the mean magnetic thickness ε, and the mean apparent magnetization $\mathfrak{m}$ and then compute the expected rms of the crustal field

$$\text{rms} = \sqrt{\sum_{l=1}^{ll} E\{R_l\}}, \tag{27}$$

to an arbitrary large maximum SH degree $ll = 10\,000$. Our least-squares misfit to the NGDC-720 spectrum consists in minimizing by trials and errors the function

$$s = \sum_{l_{\min}}^{l_{\max}} [\ln(R_l) - \ln(E\{R_l\})]^2, \tag{28}$$

as advocated by Voorhies *et al.* (2002 their eq. 14a). By doing so, we make the strong but classical assumption that the forward model $E\{R_l\}$ is known exactly and that the *a posteriori* error estimates are due to random observation errors. We also tried to adopt a probabilistic viewpoint for solving the inverse problem (e.g. Lhuillier *et al.* 2011) by taking into account the natural statistical fluctuations of the forward model. However, we are in a general statistical framework that differs from the stationary isotropic statistical model such as the one proposed by Hulot & Le Mouel (1994), for example, and we cannot apply statistical tests on individual SH degrees by treating the set $\{g_l^m\}$ as independent Gaussian centred normal variables (see the Appendix). However, we complement the misfit analysis in eq. (28) with a Kolmogorov–Smirnov (K–S) test to verify that the residuals $\ln(R_l) - \ln E\{R_l\}$ follow a normal law with the standard deviation estimated *a posteriori*. By doing so, we assume that the observation errors affect equally all SH degrees. As far as this paper is concerned, finding some sets of parameters with physically relevant values and corresponding to misfit residuals between observation and model that pass the K–S test will be considered as satisfying enough.

The 3-D surface misfit functions was calculated for parameters belonging to the intervals $\mathfrak{m} \in [0, 4]$, $\varepsilon \in [0, 110]$, and $\gamma \in [0, 3]$ for $l_{\min} = 16$ to $l_{\max} = 720$. The function is shown for restricted intervals in the Fig. 3 (in a logarithmic colour scale for illustration purposes). The global maximum likelihood values found by misfit are $\gamma \simeq 1.48$, $\varepsilon \simeq 21$ km and $\mathfrak{m} \simeq 0.7$ A m^{-1} thus providing an estimated value of the rms equal to about 197 nT (eq. 27). We see in Fig. 3 that a wide range of parameters gives comparable misfit residuals and that an absolute minimum is numerically difficult to reached. Small errors in the observations can lead to a significant reorganization of the maximum likelihood values of the three parameters that have therefore large uncertainties. In this respect, the parameter γ plays a critical role. Values ranging from 1 to 2 seem all reasonable which causes large variations in the estimated values of the pair (ε,$\mathfrak{m}$). Large power law exponent values lead to low estimates of the magnetic thickness that are balanced by comparatively higher magnetization values. The inherent ambiguity in determining the

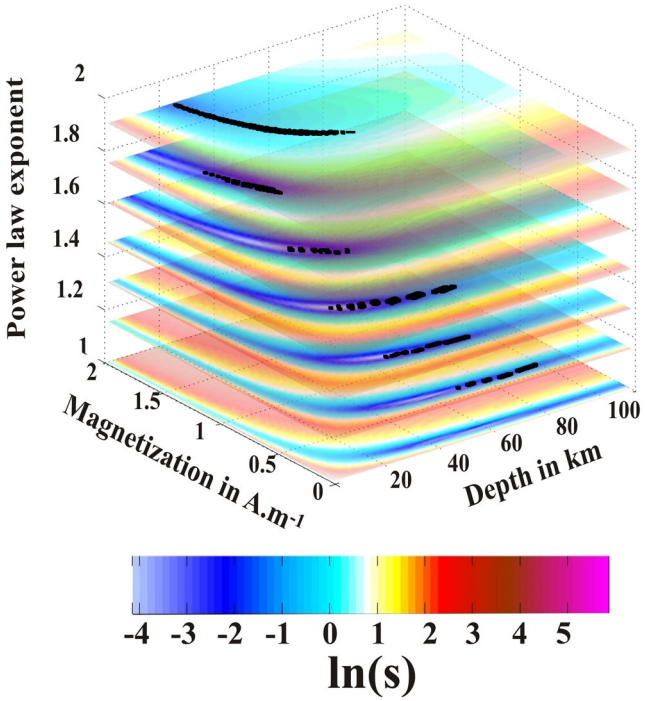

Figure 3. 3-D surface plot of the misfit defined in the eq. (28) between the observed NGDC-720 degree variance and the statistical form in logarithm scale. The black dots indicate the set of parameters for which the Kolmogorov–Smirnov test for the misfit is passed. See text for details.

three parameters, which was foreseen and discussed in Section 4, is here amplified by the observation errors and the model truncation to the SH degree 720. One satisfactory result is that the low misfit region is obtained for mean crustal thickness, magnetization, and rms that seem physically relevant considering our understanding of the Earth's magnetic crust. However, the K–S test at 95 per cent fails for all the tested parameter combinations. This could indicate that there is no statistical relationship between the observational and the statistical power spectra. However, we cannot exclude that an improbable excursion outside the normal law has occurred at some SH degree in the observation error or that the K–S failed because of the presence of outliers. We investigate in the next section whether discarding a small number of SH degrees that appear clearly as outliers allows the K–S test to be passed for some solutions.

6 STATISTICAL ANALYSES WITH PRIOR INFORMATION

6.1 Sources of errors in the observations and in the observational spectrum

The misfit analysis described above provide an objective estimate of the parameters in the absence of additional knowledge. It relies on statistical considerations and hypothesis on the error distribution that do not take into account qualitative but important metadata accompanying the different subsets constitutive of the EMAG2 grid (Maus *et al.* 2009), on which, we recall, the NGDC-720 model is based. We briefly review some possible sources of errors in order to stress that the observational power spectrum is smeared with bias.

In Fig. 4, we see some peculiarities in the shape of the NGDC-720 power spectrum. For example, the MF6 satellite model that constrains the SH degrees 16–120 of the NGDC-720 model suffers

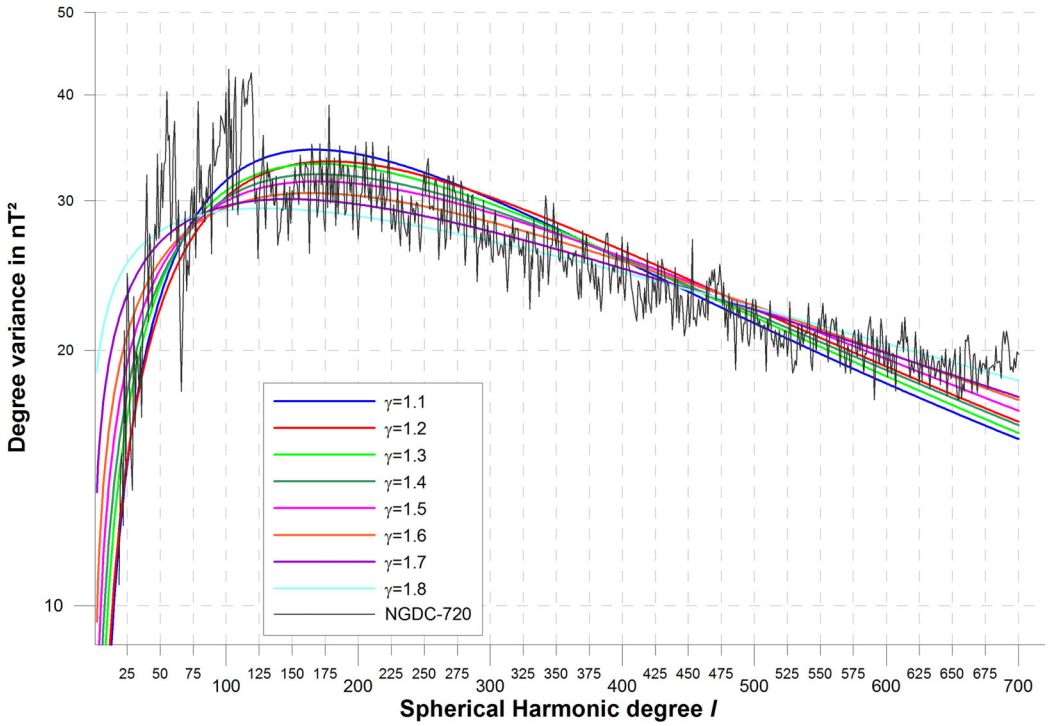

Figure 4. Best fit by trials and errors of the eq. (26) to the NGDC-720 (black curve) lithospheric field degree variance (see the text for details). The best fits are shown for different γ values varying from 1.1 to 1.8.

from a sudden drop of power from the SH degree 60 that results from a drastic data selection in the Earth's Polar areas (Maus *et al.* 2008; Thébault *et al.* 2012, for a discussion). At the other end of the power spectrum, beyond the SH degree 650, the sudden raise of the NGDC-720 power spectrum is suspicious and likely a sign of aliasing caused by the SH degree truncation. The airborne and marine magnetic data, which constrain the SH degrees larger than 120, are also corrupted by additional fill in of interpolated values and by the series of data processing applied to the data, in particular with respect to the upward/downward continuation to a common level and to the corrections for the Earth's main magnetic field at different epochs. An inspection of the EMAG2 grid further indicates that more than 10 per cent of the elements of the surface are void of airborne/marine measurements. These geographical gaps were filled with synthetic data computed to the SH degree 120 from the MF6 satellite model before the computation of the NGDC-720 model in order to mitigate the problem of ringing (see Maus 2010 for a description). Since the eq. (11) is an average over the spherical surface at the Earth's mean radius (Lowes 1966), the length scales not detected by the satellites are averaged over a surface larger than the one actually covered by the available data. This likely causes an artificial decrease of the magnetic strength for the corresponding length scales so that the SH degrees above 120 seem to have less power. A spectral gap, characterized by a loss of power is also expected for the horizontal length-scales ranging from about 200 to 450 km (between the SH degrees 90 and 200) because the nominal satellite altitude is too high and because the lateral extent of near-surface surveys is generally too small to detect robustly these features.

Other effects, however, could be more favourable to the comparison between the observational and the statistical power spectra. For example, the NGDC-720 model is built upon the EMAG2 grid values that are projected in the direction of the main field. As a result, it is by construction in agreement with our hypothesis that the lithospheric field is mostly induced by the main field. We evaluated the effect of the linearization with a synthetic analysis (not shown) and we conclude that this does not modify significantly the shape of the lithospheric field power spectrum in the waveband we consider (this property is in agreement with the views of Voorhies 1998; eq. 25a about the very small difference between the crustal magnetic field power spectra derived from random and aligned magnetization distributions). A point which is arguably more important is that the NGDC-720 global model, constructed mostly from total intensity anomalies beyond the SH degree 120, suffers from errors arising from the Backus effect (Backus 1970). This issue was addressed by minimizing the horizontal part of the magnetic field component perpendicular to the Earth's main field. Such regularization could have introduced a constrain on the shape of the lithospheric field power spectrum at large SH degrees (Maus 2010 his fig. 4).

These considerations explain why the residuals between the observational and statistical power spectrum are not random normal deviates. If before computing the K–S test we reject residual values that lie outside the 99 per cent confidence interval of the misfit distribution and if we restrict the analysis to $l_{\max} = 650$ to discard the part of the power spectrum that is possibly aliased, we obtain an ensemble of solutions that pass the K–S test (indicated as black dots in Fig. 3). The maximum likelihood is one of them. We note that the number of identified outliers in the residuals $\ln(R_l) - \ln(E\{R_l\})$ does not exceed 17 and that considering $l_{\max} = 650$ is often sufficient to pass the K–S test without outlier rejection.

The cluster of positive K–S tests in Fig. 3 is more coherent for comparatively larger values of γ. We interpret this result with caution. If we analyse the distribution of the 'outliers' for large values of γ, we note that they all belong to the waveband covered by the satellite data. This is clear also in the Fig. 4, where the statistical spectrum is skewed towards the low SH degrees for γ values ranging between 1.6 and 1.8. However, the fact that the terms up to the SH about 85 are globally more robustly determined than any other

part of the spectrum has become more or less consensual (see for instance Olsen *et al.* 2014, their fig. 5). Therefore, despite a better coherence of the K–S test for large γ values, our understanding of the data leads us to prefer the solutions obtained for γ values that allow a better fit to the waveband constrained by the satellite data. This is achieved for values lying in the range 1.3–1.5, which are also indicated as plausible by the K–S test.

From the Fig. 3 and the K–S test we conclude that the power law exponent value lies between 1 and 2 and that the crustal magnetization is confined within a shell with thickness values ranging from 10 to 80 km with a mean magnetization ranging from 0.1 to 2 A m^{-1} at 95 per cent confidence interval. If we accept some subjectivity and consider our preferred interval of γ values, these intervals reduce to values ranging from 20 to 31 km for the thickness and to 0.3 and 0.7 A m^{-1} for the mean magnetization at 95 per cent confidence interval. Apart from these large uncertainties, one salient result is that the analysis shows that the observational NGDC-720 power spectrum can be a realization of the stochastic process described by the eq. (26) for the SH degrees 16–650 and that the estimated magnetic crustal thickness, the apparent magnetization, and the root mean square of the crustal field belong to intervals of physically relevant values.

6.2 Independent estimate values for γ

We found some ensemble of parameters for which the observational Earth's lithospheric magnetic field degree variance seems to be statistically well described by the eq. (26). The mean magnetization and crustal thickness are two quantities that have a straightforward physical meaning. This is not the case of the power exponent γ that derives from the (arbitrary) assumption that the degree variance of the susceptibility follows a power law (eq. 15).

Susceptibility models of the Earth's crust do not allow obtaining the correct amplitudes or/and the shapes of the lithospheric magnetic field spatial structures (Hemant & Maus 2005). In the spectral domain, however, such limitations are less important and these models provide a mean to verify whether the assumption of power-law dependency for the susceptibility power spectrum is a reasonable one. We investigate this question on a global scale and for the continental and the oceanic domains separately.

For the global Earth, we consider the full world map of the integrated susceptibility published by Hemant & Maus (2005; the so-called H&M model hereafter). The H&M vertically integrated susceptibility grid is provided to a resolution of $0.25^\circ \times 0.25^\circ$ and was obtained by multiplying the susceptibility model by the seismic CRUST2.0 model for the crustal thickness (Bassin *et al.* 2000; http://igppweb.ucsd.edu/~gabi/crust2.html). The coefficients χ_l^m in the eq. (10) being those for the apparent susceptibility in SI unit (not the vertically integrated one in SI.km unit) we therefore divide the H&M susceptibility grid by the CRUST2.0 model to obtain a comparable quantity. We then convert the grid in SHs to the SH degree 500 by a fast spherical transform and compute the slope of the power spectrum (eq. 14) in a log–log scale by least-squares fit. For the global Earth, we verify that the power spectrum follows a power law with $\gamma \simeq 1.36 \pm 0.08$, which is a value that falls within the possible power-law exponents found by the misfit analysis (eq. 28). The errors bars on γ correspond to the 95 per cent confidence interval.

For the continental crust, we first compute the susceptibility values on the nodes of a global Fourier–Gauss grid. Then, a map of the shorelines (including the submarine continental crusts) is used to set the boundary between the continental and the oceanic domains and null susceptibility values are set in the oceanic domain. After the conversion of the continental grid in SH to the degree 500 and the computation of the susceptibility power spectrum, we again verify that the power spectrum follows a power law and we find by least-squares fit that $\gamma \simeq 1.34 \pm 0.04$. Turning now to the oceanic domain, we perform a similar analysis using different models for the remanent magnetization of the ocean floors. Dyment & Arkani-Hamed (1998) propose three models computed with mean magnetizations equal to 16, 4 and 2.75 A m^{-1} and crustal thickness equal to 0.5, 12 and 30 km, respectively. They indicate their preference to the map built with a magnetization of 4 A m^{-1} and a crustal thickness of 12 km. Their maps are integrated over the entire thickness (Vertically Integrated Magnetization, VIM) and give the module of the magnetization with the sign of the polarity of the Earth's palaeomagnetic field. We roughly convert each map into an equivalent susceptibility grid by dividing the VIM values by the respective (constant) crustal thickness. We then change the polarity of the grid in the Southern hemisphere (in order to account for the polarity change of the Earth's main dipole field from one hemisphere to the other) and finally transform the grids into an equivalent set of susceptibility parameters to the SH degree 500. For the first grid (16 A m^{-1}, 0.5 km), we do not estimate the power law exponent because the spectrum is not straight in a log–log scale (DA0.5_16 in Fig. 5, black curve). For the second grid (4 A m^{-1}, 12 km), we find a power spectrum following a power law with $\gamma \simeq 1.40 \pm 0.09$ (DA12_4.0 in Fig. 5, green curve) and for the third (2.75 A m^{-1}, 30 km) we find $\gamma \simeq 1.44 \pm 0.08$ (DA30_2.7 in Fig. 5, orange curve). Recently, Masterton *et al.* (2012, the MAS model) published a model combining the vertically integrated susceptibility of H&M and an independent model of ocean floors magnetization. We extract the VIM for the ocean and divide it by the CRUST2.0 model in order to retrieve a magnetization in the unit of A m^{-1}. Again, we convert this map into SH apparent susceptibility coefficients to degree 500 and estimate $\gamma \simeq 1.36 \pm 0.07$ (MAS in Fig. 5 magenta curve). These three models for the ocean floors provide different maximum likelihood values for γ but with some overlap between their 95 per cent confidence intervals. For the oceanic domain, we will consider hereafter values of γ ranging from 1.29 to 1.49, which are the extrema of the 95 per cent confidence interval of the ensemble of the three models.

An important result emerging from this analysis is that these independent models for the susceptibility and magnetization have power spectra in SH that follow well the assumption of a single power law between the SH degrees 16 and 650. All the power law values estimated from these independent models incidentally belong to the preferred interval that we found by misfit analysis of the NGDC-720 degree variance (between $\gamma = 1.3$ and 1.5) and are comparable to the estimated maximum likelihood value ($\gamma \simeq 1.48$). This gives us some confidence that the exponent value γ in eq. (26) that was introduced *a priori* without firm physical arguments is not a dummy parameter but is a relevant variable in our problem. We have not yet elucidated its physical significance (if any) but we stress that finding that the susceptibility power spectrum indeed follows a power law is not sufficient (and not the scope of this study) to confirm that the susceptibility is self-similar in space.

6.3 The mean magnetization and magnetic crustal thickness

Having estimated power-law values from independent models, we now constrain the value of γ in the misfit analysis (eq. 28) in order to

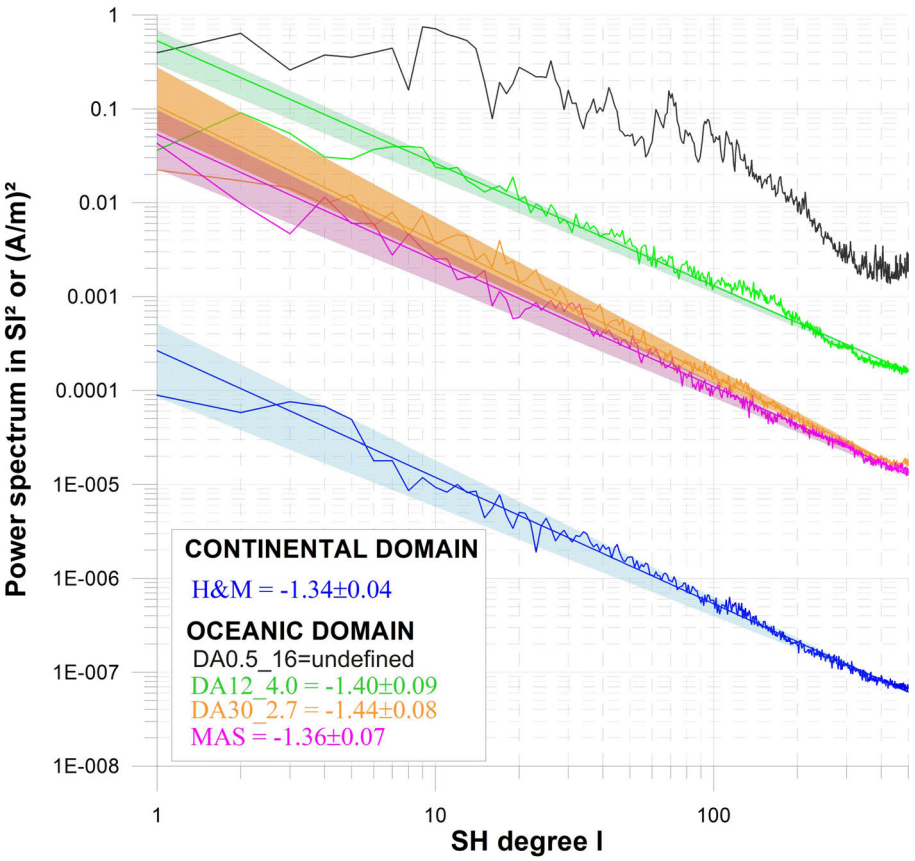

Figure 5. The spherical harmonic degree variances of the susceptibility distribution (H&M in blue) of Hemant & Maus (2005), of the three equivalent susceptibility maps derived from the magnetization models in the oceans (DA12_4.0 in light green, DA0.5_16 in black, and DA30_2.7 in orange) of Dyment & Arkani-Hamed (1998), and of the equivalent susceptibility derived from the magnetization map for the oceans (MAS in magenta) of Masterton *et al.* (2012). The degree variances are displayed in a log–log scale. Straight lines are the power law estimation with their 95 per cent confidence intervals. The power exponents are indicated in the boxcar.

better bound the estimates for the mean magnetic crustal thickness and magnetization. We perform the analysis globally and for the continental and the oceanic domains.

For the global Earth, γ is restricted to the interval $\gamma \simeq 1.36 \pm 0.08$ as was found from the H&M susceptibility model. With this constrain on γ, the magnetic crustal thickness value is found to be between 23 and 30 km at 95 per cent confidence interval, the magnetization value between about 0.3 and 0.6 A m^{-1}, and the rms between 190 and 205 nT.

We now investigate the performance of the statistical degree variance on large regional scales. By doing so we implicitly make use of the assumption that the lithospheric field is the realization of a stationary process. We split the magnetic field contributions of the NGDC-720 model into the oceanic and the continental domains. We proceed as previously and first compute the magnetic contributions on the nodes of a Fourier–Gauss grid. Then, a map of the shorelines (including the submarine continental crusts) is used to set the boundary between both domains and null magnetic field values are set in the complement of the oceanic or of the continental domain, respectively. Finally, we estimate the individual degree variance up to the SH degree 720 using a spherical transform algorithm.

The Fig. 6 shows the NGDC-720 degree variance and its decomposition into both domains to the SH degree 650. Qualitatively, the magnetic field over the continents dominates the total degree variance up to the SH degree 125. There is next a competing region between the oceanic and the continental crusts to the SH degree 220 from which the oceanic signal dominates the global degree variance. Interestingly, the degree variance is regular for the oceanic regions despite an incomplete global geographical data coverage over the oceans. One explanation would be that the oceanic magnetic crust is structurally homogeneous at these length scales (similar mean thickness, composition, and magnetization) and that the signals missing cause a mere depletion of the total degree variance. This effect is easily conceived if we consider that the ocean magnetic field anomalies are massively produced by magnetized structures parallel to the ridges. As second possible explanation comes from the fact that the parent EMAG2 grid of the NGDC-720 model was constructed with an interpolation scheme based on the direction of the isochrons in the ocean floors. Therefore, we cannot rule out that the regularity of the magnetic field spatial power spectrum in the oceans is partly imposed by the gridding algorithm.

The same regularity is not observed over continents. A certain level of variability is expected if the regional variations of the mean magnetization, the crustal thickness, and the power law for the susceptibility are significant within the continental magnetic crust. In such a case, the power spectrum over continents can be seen as the linear superimposition of regional power spectra obeying the same statistical process but with different regional magnetization, crustal thickness, and asymptotic behaviours. However, the missing data over portions of large regions like Antarctica, South America or Africa (see e.g. Maus *et al.* 2009 their fig. 7) could also cause artificial loss of power at different wavebands and therefore explain

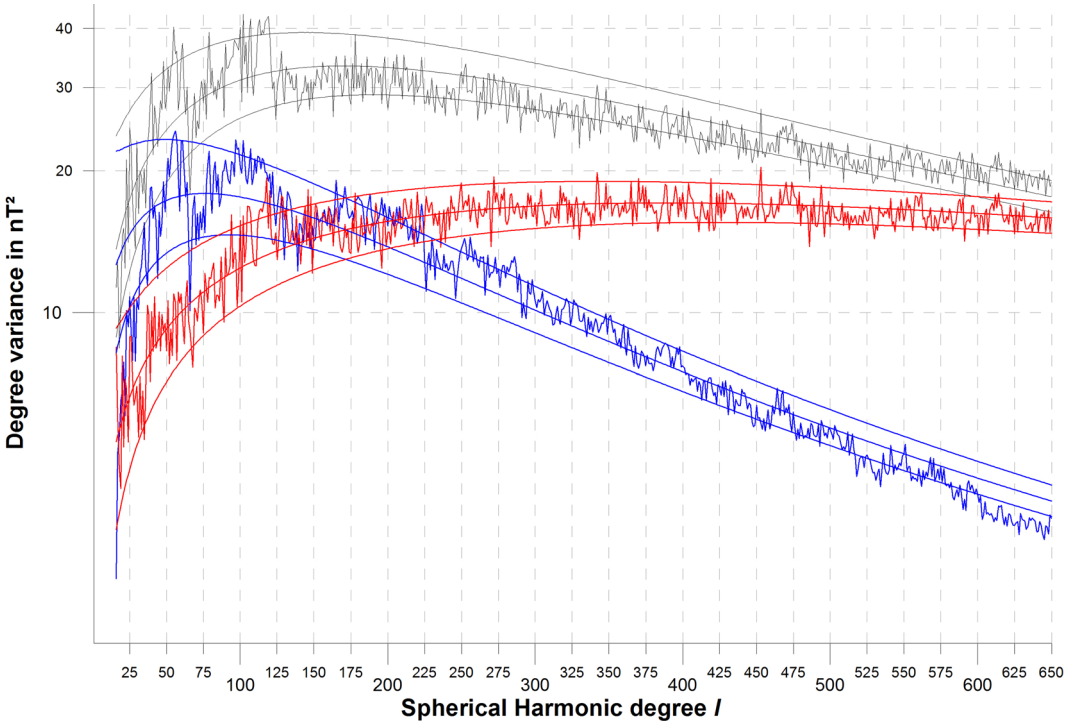

Figure 6. The degree variance of the NGDC-720 model (black) is separated into its contributions into continental (blue) and oceanic (red) domains to the SH degree 650. The solid curves are the statistical degree variances (eq. 26) best fitting each observed spectrum with the power law exponent γ indicated in the text. The 95 per cent confidence intervals are also indicated.

some of the observed breaks in the power spectrum (between the SH 125 and 175 or 222 and 250, for instance). It is also clear from the power spectrum on continents that missing aeromagnetic data over large areas cause a strong loss of energy starting from the SH degree 120.

The misfit analyses by the eq. (28) in both domains are quantitatively encouraging. For the continents, we use the interval $\gamma \simeq 1.34 \pm 0.04$ found from the analysis of the H&M susceptibility model. The multivariate distribution indicates that the crustal thickness value lies between 55 and 65 km and that the magnetization is between 0.1 and 0.3 A m^{-1} at 95 per cent. Without *a priori* information on γ we find by misfit the maximum likelihood for the continents $\gamma = 1.26$, $\varepsilon = 63$ km and $\mathrm{m} = 0.1$ A m^{-1}. The K–S test is not passed, which can cast doubts on the ability of the statistical power to explain the observed one on continents. However, this failure could also indicate that the assumed statistics on the error is wrong over continents because of large data gaps at the global scale as was described above. We remind that the artificial loss of power at SH degree larger than about 120 (as a result of the incomplete near-surface data coverage) can lead to the overestimation of the crustal thickness and the underestimation of the mean magnetization and we should probably not give too much credit to the numerical mean values found for the continents.

For the oceans, a similar analysis considering now γ ranging from 1.29 to 1.49 indicates that the crustal thickness is between 6 and 15 km and the magnetization between 0.4 and 1.8 A m^{-1} at 95 per cent confidence interval. Without any *a priori* on the value of γ, we find a best misfit to the NGDC-720 model for $\gamma = 1.44$, $\varepsilon = 11$ km and $m = 1.1$ A m^{-1}. In this case, the power law estimated from the magnetic field degree variance over oceans belongs to the confidence interval of the three independent magnetization models of the ocean floors. The K–S test is also passed for some combination of parameters (including the maximum likelihood values) in oceans showing that we cannot reject the idea that the observational power spectrum on oceans can be a realization of the stochastic process.

In Fig. 6 we display the maximum likelihood statistical power spectra for each domain with their 95 per cent confidence interval. The interval is built numerically and corresponds to the 95 per cent envelope of 10 000 random samples of the statistical power spectrum each computed using the maximum likelihood parameters. The observational and statistical power spectra over oceans are in particularly good agreement at all scales. We might be tempted to consider this result as physically irrelevant because there is no evidence that the induced magnetic field dominates over the remanent magnetic field in oceans but we recall that the NGDC-720 model is built upon a grid of scalar values that are projected in the direction of the main field and is by construction in agreement with the induced field hypothesis. We also argue that the induced and remanent magnetization share similar statistics at these length scales (see also Voorhies 1998). Over continents, we see an increasing number of SH degrees of the observational power spectrum lying outside the 95 per cent confidence interval of the statistical spectrum. We notice clear outlier values (from SH degree 65 and beyond SH degree 650, for instance) that explain partly the failure of the K–S test. However, the general shapes of the observational and statistical spectra remain in good visual agreement.

7 DISCUSSION AND CONCLUSIONS

We derived a statistical expression for the lithospheric magnetic field degree variance from simple principles in terms of laterally varying susceptibility in a shell of constant thickness. We introduced supplementary assumptions on the susceptibility in the spectral domain and imposed that its SH power spectrum follows a power law. This allowed us to bypass the intricate problem that consists in defining a idealized correlation function for the sources in the spatial domain.

We obtained a form in function of three free parameters: the thickness of the magnetized shell, the mean apparent magnetization, and a power-law exponent for the power spectrum of the susceptibility.

The relevance of this statistical form was tested against the NGDC-720 model (Maus 2010) which currently provides the unique published description of the lithospheric magnetic field to large SH degrees. We performed misfit analyses on the spectrum of the global NGDC-720 model and also for the spectra in the oceanic and continental domains separately. The goodness of fit was tested using the classical K–S test. This test suggests that the data support the physics and the statistics assumed in this paper for the power spectrum of the lithospheric field at the global scale and in the oceanic domain. This is not the case for continents but we consider that the failure of the K–S test is not sufficient to rule out the proposed statistical model because we do not know enough the distribution of the errors in the spectrum for the SH degrees larger than 120.

Other criteria are to be considered. We find that the estimated values for the mean crustal thickness, the mean magnetization, and the root mean square of the crustal field have physically relevant values. Their comparison with those estimated via independent models is in some cases striking. The mean seismic crustal thickness derived from the CRUST2.0 seismic model (Bassin *et al.* 2000; http://igppweb.ucsd.edu/~gabi/crust2.html) is equal to about 21 or 23 km considering the recent CRUST1.0 model (Laske *et al.* 2013) while we estimated by misfit that the mean magnetic crustal thickness value is between 23 and 30 km at 95 per cent confidence interval. This good agreement supports the assumption that the Moho depth is statistically (or globally) a thermal boundary for the lithospheric magnetic field (Wasilewski & Mayhew 1992). The mean magnetization of the crust varies greatly with the composition of the crust but we note that the mean estimated value (between 0.3 and 0.6 A m^{-1}) also compares favourably with typical measured values (for instance, Hahn & Roeser 1989) or values estimated by regional or global analyses (Whaler & Langel 1996; Thébault *et al.* 2010 their fig. 9; Masterton *et al.* 2012). In addition, the relative difference in magnetization and thickness between the oceans and continents is intuitively satisfying. It confirms that the magnetic continental crust is thicker than the oceanic crust. The separation of the CRUST2.0 seismic map into continental and oceanic domains indicates a crustal thickness of 37 km and 10 km, respectively. The mean seismic and magnetic crustal (between 6 and 15 km) thickness values in oceans are in good agreement whereas, again, a discrepancy that we explain mostly by the incompleteness of the magnetic data is found for continents (between 55 and 65 km). The relative difference in magnetization for the continental (0.1–0.3 A m^{-1}) and oceanic (0.4–1.8 A m^{-1}) crusts can be interpreted as the difference of composition between the main magnetic carriers (basaltic or granitic) in both domains. The interpretation of the power law for the susceptibility power spectrum is not as straightforward as the mean crustal thickness and magnetization. However, we could show that the values estimated by the magnetic data and independent models were also in good agreement. Considering the general level of approximation embedded in such world magnetization/susceptibility maps, and the level of accuracy of the global magnetic data set, the overall consistency is remarkable. All these indicators give us some confidence that the statistical expression we propose is not in contradiction with the NGDC-720 lithospheric magnetic field model or with the independent world models for the SH degrees 16–650. Of course, they do not prove the validity of the underlying assumptions. The statistical solution does not resolve the ambiguity about the nature (induced or remanent) and the formation process of the magnetic sources nor does it exclude the presence of magnetic carrier locally down to the upper mantle (Ferré *et al.* 2014). The regional interpretations of the magnetic anomalies in terms of susceptibility only (e.g. Arkani-Hamed & Strangway 1985), of crustal thickness (e.g. Bouligand *et al.* 2009), or in terms of heat flow anomalies (e.g. Rajaram *et al.* 2009) remain legitimate. Statistically, however, the observational power spectrum can be represented by a simple model of three parameters such as the mean magnetization, the mean magnetic crustal thickness, and a single power law index for the susceptibility power spectrum.

If we accept that the observational degree variance of the lithospheric field could be a realization of the statistical model discussed in this paper, a primary feature that emerges is that we expect it to follow two distinct regimes. The first regime is defined for the large wavelengths and is well described by an equivalent layer of magnetization with finite and constant thickness that modulates the degree variance. It is characterized by a maximum at a SH degree that is a function of the mean crustal thickness. The second regime becomes apparent after the peak of the magnetic spectrum has been reached but dominates clearly only at very high SH degrees. This regime is dominated by the susceptibility spectrum that produces asymptotically a quasi-constant slope in the magnetic field power spectrum in a log–log scale (Fig. 1). This indicates that the magnetic field power spectrum could show a fictitious power-law dependency at relatively large wavenumbers but that it is curvy in general.

Finally, the statistical form provides an interesting insight into the practical difficulties of estimating the crustal thickness, the magnetization, and the power law of the susceptibility from magnetic field spectral analyses. The depth can be estimated after the identification of the maximum of the degree variance. For crustal thickness of a few tenths of kilometres, for instance, we predict that the magnetic spectrum reaches its maximum between the SH degrees 50 and 200 (see for instance the degree variance over the continents in Fig. 6). Such spatial scales are hardly detected by near-surface and satellites surveys so this parameter is globally poorly constrained by the available data. Conversely, we predict that the maximum of the power spectrum shifts towards the large SH degrees when the depth is shallower but that it spreads at the same time over a wide range of SH degrees (see for instance the degree variance over the oceans in Fig. 6). In such a case, its identification is challenging if the data are not homogeneous and accurate over a large waveband. Turning now to the mean apparent magnetization, we may consider easier its identification because it plays the role of a simple multiplicative factor in the power spectrum. However, its estimation requires that the observational power spectrum is also computed carefully from a homogeneous data set because any lack of data or excess of power will modify its mean value. The overall solution is sensitive to this parameter and in Fig. (3) we see that small uncertainties on the mean magnetization value lead to large errors on the mean crustal thickness. At last, the power law exponent is a parameter that is best constrained at (very) large SH degrees when the crustal field power spectrum reaches its quasi-constant slope regime. A decent estimation of this parameter thus requires a global data set depicting the Earth's crustal field to a few kilometres resolution and therefore this parameter is the most uncertain.

We cannot ascertain that the NGDC-720 observational power spectrum is reliable over its entire range and we cannot rule out that the overall consistency we observe could be fortuitous. Further tests on independent global and regional models will be necessary to assess the validity of the proposed spectral form. Keeping this in mind, the spectral form for the lithospheric field power spectrum could be exploited at different levels in geomagnetism. For example, the complementary analyses we performed in the continental

and the oceanic domains suggest that the same approach could be applied on regional scales for investigating the regional variability of the magnetic crustal thickness, the magnetization and the scaling exponent for the susceptibility in regions where data constrain a wide range of spatial scales. This opens an avenue for the estimation of large spatial scales of the Earth's magnetic crustal thickness (see Lewis & Simons 2012 for an attempt on Mars) that are not directly accessible from the magnetic field measurements. However, this would require considering the oblateness of the Earth. This could be done by relying on regional modelling schemes that have been developed in the framework of geomagnetism (see Schott & Thébault 2011 for a review). Such a worldwide analysis could be based on frames of Poisson wavelets (e.g. Maier & Mayer 2003), on Slepian functions (e.g. Beggan *et al.* 2013), on combination of band-limited SHs (e.g. Lesur 2006), or on revised spherical cap harmonic analysis (Thébault 2008), for instance.

The statistical form can also be useful for bounding the large lithospheric field wavelengths overlapping with the core field (Jackson 1996). In particular, the spectral form discussed in this paper is more energetic at the low SH degrees than the ones previously published (Jackson 1990, 1994; Voorhies 1998; Voorhies *et al.* 2002). This suggests that the main field modelling error caused by the crustal field could have been so far underestimated (see Baerenzung *et al.* 2014, for a recent consideration of the crustal field error). This aspect is important in the framework of geomagnetic data assimilation whose aim is to estimate the state vector of the Earth's outer core flow but that requires suitable error covariance matrices on the magnetic observations or on the core field models at low SH degrees (Fournier *et al.* 2011). Such covariance matrices can be readily estimated by the formula given in the Appendix.

Beyond the scope of geomagnetism, the exponent value for the magnetic susceptibility over continents and oceans is intriguing. For the continents, the power law $\gamma = 1.36 \pm 0.07$ of the H&M model compares well with the self-similarity of fragmentation estimated by Turcotte (1986) and one may venture that it could characterize the geological evolution of the crustal rock properties. This tantalizing analogy between the fragmentation and the Earth's crust deformation by tectonic processes suggests that large-scale magnetics could help to understand the dynamic process of plate tectonics. It is difficult to provide a rigorous theoretical framework accounting for this power law value but a systematic investigation of power laws combined with deterministic equations might nevertheless be rewarding and help reconciling geophysical topics that are often disconnected.

ACKNOWLEDGEMENTS

This work was partly funded by the Centre National des Etudes Spatiales (CNES) within the context of the project of the 'Travaux préparatoires et exploitation de la mission Swarm'. FV was funded by the Région Ile de France. We would like to thank K. Hemant for providing the susceptibility map of the world, J. Dyment for providing the magnetization models of the ocean floors and S. Masterton for sharing the grid for the world vector magnetization. We would like to thank the editor R. Holme, the reviewer C.V. Voorhies, and an anonymous reviewer who helped us to improve this manuscript. This is IPGP contribution number 3589.

REFERENCES

Arkani-Hamed, J. & Strangway, D.W., 1985. Lateral variations of apparent magnetic susceptibility of lithosphere deduced from Magsat data, *J. geophys. Res.,* **90**(B3), 2655–2664.

Backus, G., 1970. Non-uniqueness of the external geomagnetic field determined by surface intensity measurements, *J. geophys. Res.,* **75**(31), 6339–6341.

Backus, G., Parker, R.L. & Constable, C., 1996. *Foundations of Geomagnetism,* Cambridge Univ. Press.

Baerenzung, J., Holschneider, M. & Lesur, V., 2014. Bayesian inversion for the filtered flow at the Earth's core-mantle boundary, *J. geophys. Res.,* **119**(4), 2695–2720.

Bassin, C., Laske, G. & Masters, G., 2000. The current limits of resolution for surface wave tomography in North America, *EOS, Trans. Am. geophys. Un.,* **81**(48), F897, Abstract S12A-03.

Beggan, C.D., Saarimäki, J., Whaler, K.A. & Simons, F.J., 2013. Spectral and spatial decomposition of lithospheric magnetic field models using spherical Slepian functions, *Geophys. J. Int.,* **193**(1), 136–148.

Blakely, R.J., 1995. *Potential Theory in Gravity and Magnetic Applications,* Cambridge Univ. Press.

Bouligand, C., Glen, J.M.G. & Blakely, R.J., 2009. Mapping Curie temperature depth in the western United States with a fractal model for crustal magnetization, *J. geophys. Res.,* **114,** B11104, doi:10.1029/2009JB006494.

Counil, J., Cohen, Y. & Achache, J., 1991. The global continent–ocean magnetisation contrast: spherical harmonic analysis, *Earth planet. Sci. Lett.,* **103,** 354–364.

Dyment, J. & Arkani-Hamed, J., 1998. Contribution of lithospheric remanent magnetization to satellite magnetic anomalies over the world's oceans, *J. geophys. Res.,* **103**(B7), 15 423–15 441.

Ferré, E.C., Friedman, S.A., Martín-Hernández, F., Feinberg, J.M., Till, J.L., Ionov, D.A. & Conder, J.A., 2014. Eight good reasons why the uppermost mantle could be magnetic, *Tectonophysics,* **624,** 3–14.

Fournier, A., Aubert, J. & Thébault, E., 2011. Inference on core surface flow from observations and 3-D dynamo modelling, *Geophys. J. Int.,* **186**(1), 118–136.

Fox Maule, C., Purucker, M., Olsen, N. & Mosegaard, K., 2005. Heat flux anomalies in Antarctica revealed by satellite magnetic data, *Science,* **309,** 464–467.

Gubbins, D., Ivers, D., Masterton, S.M. & Winch, D.E., 2011. Analysis of lithospheric magnetization in vector spherical harmonics, *Geophys. J. Int.,* **187,** 99–117.

Hahn, A.G. & Roeser, H.A., 1989. The magnetisation of the lower continental crust, in *Properties and Processes of Earth' Lower Crust, Geophys. Monogr. Ser.,* Vol. 51, pp. 247–253, eds Mereu, R.F., Mueller, S. & Fountain, D.M., AGU.

Hamoudi, M., Thébault, E., Lesur, V. & Mandea, M., 2007. GeoForschungsZentrum Anomaly Magnetic Map (GAMMA): a candidate model for the world digital magnetic anomaly map, *Geochem. Geophys. Geosyst.,* **8,** Q06023, doi:10.1029/2007GC001638.

Hemant, K. & Maus, S., 2005. Geological modeling of the new CHAMP magnetic anomaly maps using a Geographical Information System (GIS) technique, *J. geophys. Res. B,* **110,** B12103, doi:10.1029/2005JB003837.

Hemant, K., Thébault, E., Mandea, M., Ravat, D. & Maus, S., 2007. Magnetic anomaly map of the world: merging satellite, airborne, marine and ground-based magnetic data sets, *Earth planet. Sci. Lett.,* **260,** 56–71.

Hulot, G. & Le Mouel, J.-L., 1994. A statistical approach to the Earth's main magnetic field, *Phys. Earth planet. Inter.,* **82**(3), 167–184.

Hulot, G., Olsen, N. & Sabaka, T.J., 2007. The present field, in *Treatise on Geophysics,* Chapter 6, Vol. 5: Geomagnetism, pp. 33–72, ed. Kono, M., Elsevier.

Jackson, A., 1990. Accounting for crustal magnetization in models of the core magnetic field, *Geophys. J. Int.,* **103,** 657–673.

Jackson, A., 1994. Statistical treatment of crustal magnetization, *Geophys. J. Int.,* **119,** 991–998.

Jackson, A., 1996. Bounding the long-wavelength crustal magnetic field, *Phys. Earth planet. Inter.,* **98,** 283–302.

Korhonen, J.K. *et al.*, 2007. *Magnetic Anomaly Map of the World - Carte des anomalies magnétiques du monde, Scale: 1:50,000,000,* 1st edition. Commission for the Geological Map of the World.

Kotsiaros, S. & Olsen, N., 2014. End-to-End simulation study of a full magnetic gradiometry mission, *Geophys. J. Int.,* **196,** 100–110.

Langel, R.A. & Estes, R.H., 1982. A geomagnetic field spectrum, *Geophys. Res. Lett.,* **9,** 250–253.

Langel, R.A. & Hinze, W.J., 1998. *The Magnetic Field of the Earth's Lithosphere: The Satellite Perspective,* 429 pp., Cambridge Univ. Press.

Laske, G., Masters, G., Ma, Z. & Pasyanos, M., 2013. Update on CRUST1.0—a 1-degree Global Model of Earth's Crust, *J. geophys. Res.,* Abstracts, 15, Abstract EGU2013-2658.

Lesur, V., 2006. Introducing localized constraints in global geomagnetic field modelling, *Earth Planets Space,* **58,** 477–483.

Lewis, K.W. & Simons, F.J., 2012. Local spectral variability and the origin of the Martian crustal magnetic field, *Geophys. Res. Lett.,* **39,** L18201, doi:10.1029/2012GL052708.

Lhuillier, F., Fournier, A., Hulot, G. & Aubert, J., 2011. The geomagnetic secular-variation timescale in observations and numerical dynamo models, *Geophys. Res. Lett.,* **38**(9), L09306, doi:10.1029/2011GL047356.

Lovejoy, S., Pecknold, S. & Schertzer, D., 2001. Stratified multifractal magnetization and surface geomagnetic fields—I. Spectral analysis and modelling, *Geophys. J. Int.,* **145**(1), 112–126.

Lowes, F.J., 1966. Mean square values on the sphere of spherical harmonic vector fields, *J. geophys. Res.,* **71,** 2179.

Lowes, F.J., 1974. Spatial power spectrum of the main geomagnetic field and extrapolation to the core, *Geophys. J. R. astr. Soc.,* **36,** 717–730.

Maier, T. & Mayer, C., 2003. Multiscale downward continuation of CHAMP FGM-data for crustal field modelling, in *First CHAMP Mission Results for Gravity, Magnetic and Atmospheric Studies,* pp. 288–295, eds Reigber, C., Lühr, H. & Schwintzer, P., Springer-Verlag.

Masterton, S., 2010. Modelling and interpretation of magnetisation in the oceanic lithosphere, *PhD thesis,* School of Earth and Environment, University of Leeds, UK.

Masterton, S., Gubbins, D., Müller, R.D. & Singh, K.H., 2012. Forward modelling of oceanic lithospheric magnetization, *Geophys. J. Int.,* **192**(3), 951–962.

Maus, S., 2008. The geomagnetic power spectrum, *Geophys. J. Int.,* **174**(1), 135–142.

Maus, S., 2010. An ellipsoidal harmonic representation of Earth's lithospheric magnetic field to degree and order 720, *Geochem. Geophys. Geosyst.,* **11,** Q06015, doi:10.1029/2010GC003026.

Maus, S. & Dimri, V.P., 1994. Scaling properties of potential fields due to scaling sources, *Geophys. Res. Lett.,* **21**(10), 891–894.

Maus, S. & Haak, V., 2002. Is the long wavelength crustal magnetic field dominated by induced or by remanent magnetisation?, *J. Ind. Geophys. Un.,* **6**(1), 1–5.

Maus, S., Gordon, D. & Fairhead, D., 1997. Curie temperature depth estimation using a self-similar magnetization model, *Geophys. J. Int.,* **129,** 163–168.

Maus, S., Sazonova, T., Hemant, K., Fairhead, J.D. & Ravat, D., 2007. National Geophysical Data Center candidate for the World Digital Magnetic Anomaly Map, *Geochem. Geophys. Geosyst.,* **8,** Q06017, doi:10.1029/2007GC001643.

Maus, S. *et al.*, 2008. Resolution of direction of oceanic magnetic lineations by the sixth-generation lithospheric magnetic field model from CHAMP satellite magnetic measurements, *Geochem. Geophys. Geosyst.,* **9,** Q07021, doi:10.1029/2008GC001949.

Maus, S. *et al.*, 2009. EMAG2: A 2–arc min resolution Earth Magnetic Anomaly Grid compiled from satellite, airborne, and marine magnetic measurements, *Geochem. Geophys. Geosyst.,* **10,** Q08005, doi:10.1029/2009GC002471.

Mayhew, M.A., 1985. Curie Isotherm Surfaces Inferred From High-Altitude Magnetic Anomaly Data, *J. geophys. Res.,* **90**(B3), 2647–2654.

O'Brien, M.S., Parker, R.L. & Constable, C.G., 1999. Magnetic power spectrum of the ocean crust on large scales, *J. geophys. Res.,* **104**(B12), 29 189–29 201.

Olsen, N., Luehr, H., Finlay, C.C., Sabaka, T.J., Michaelis, I., Rauberg, J. & Toeffner-Clausen, L., 2014. The CHAOS-4 Geomagnetic Field Model, *Geophys. J. Int.,* **197,** 815–827.

Pilkington, M. & Todoeschuck, J.P., 1993. Fractal magnetization of continental crust, *Geophys. Res. Lett.,* **20**(7), 627–630.

Pilkington, M. & Todoeschuck, J.P., 1995. Scaling nature of crustal susceptibilities, *Geophys. Res. Lett.,* **22**(7), 779–782.

Purucker, M. & Whaler, W., 2007. Crustal magnetism, in *Treatise on Geophysics,* Chapter 6, Vol. 5: Geomagnetism, pp. 195–237, ed. Kono, M., Elsevier.

Purucker, M., Langlais, B., Olsen, N., Hulot, G. & Mandea, M., 2002. The southern edge of cratonic North America: evidence from new satellite magnetometer observations, *Geophys. Res. Lett.,* **29**(15), doi:10.1029/2001GL013645.

Rajaram, M., Anand, S.P., Hemant, K. & Purucker, M.E., 2009. Curie isotherm map of Indian Subcontinent from Satellite and Aeromagnetic Data, *Earth planet. Sci. Lett.,* **281,** 147–158.

Reigber, C.H. & Lühr, S.P., 2002. CHAMP Mission Status, *Adv. Space Res.,* **30**(2), 129–134.

Runcorn, S.K., 1975. On the interpretation of Lunar magnetism, *Phys. Earth planet. Int.,* **10,** 327–335.

Rygaard-Hjalsted, C., Constable, C.G. & Parker, R.L., 1997. The influence of correlated crustal signals in modelling the main geomagnetic field, *Geophys. J. Int.,* **130**(3), 717–726.

Schott, J.J. & Thébault, E., 2011. Modelling the Earth's magnetic field from global to regional scales, in *Geomagnetic Observations and Models,* IAGA Special Sopron Book Series, Vol. 5, pp. 229–264, eds Mandea, M. & Korte, M., Springer.

Spector, A. & Grant, S., 1970. Statistical models for interpreting aeromagnetic data, *Geophysics,* **35,** 293–302.

Thébault, E., 2008. A proposal for regional modelling at the Earth's surface, R-SCHA2D, *Geophys. J. Int.,* **174**(1), 118–134.

Thébault, E., Hemant, K., Hulot, G. & Olsen, N., 2009. On the geographical distribution of induced time-varying crustal magnetic fields, *Geophys. Res. Lett.,* **36,** L01307, doi:10.1029/2008GL036416.

Thébault, E., Purucker, M., Whaler, K., Langlais, B. & Sabaka, T.J., 2010. The magnetic field of the Earth's lithosphere, *Space Sci. Rev.,* **155**(1–4), 95–127.

Thébault, E., Vervelidou, F., Lesur, V. & Hamoudi, M., 2012. The along-track satellite analysis in planetary magnetism, *Geophys. J. Int.,* **188**(3), 891–907.

Turcotte, D.L., 1986. Fractals and fragmentation, *J. geophys. Res.,* **91**(B2), 1921–1926.

Vervelidou, F., 2013. Contribution à la modélisation et à l'interprétation multi-échelle du champ magnétique de la lithosphère terrestre, *PhD thesis,* Institut de Physique du Globe de Paris, Unvi. Paris Diderot, France.

Voorhies, C.V., 1998. *Elementary theoretical forms for the spatial power spectrum of Earth's crustal magnetic field, NASA Tech. Pap. 1998-208608,* 38 pp.

Voorhies, C.V., Sabaka, T.J. & Purucker, M., 2002. On magnetic spectra of Earth and Mars, *J. geophys. Res.,* **107,** 5034, doi:10.1029/2001JE001534.

Wasilewski, P.J. & Mayhew, M.A., 1982. Crustal xenolith magnetic properties and long wavelength anomaly source requirements, *Geophys. Res. Lett.,* **9**(4), 329–332.

Wasilewski, P.J. & Mayhew, M.A., 1992. The Moho as a magnetic boundary revisited, *Geophys. Res. Lett.,* **19**(22), 2259–2262.

Whaler, K.A. & Langel, R.A., 1996. Minimal crustal magnetizations from satellite data, *Phys. Earth planet. Inter.,* **98,** 303–319.

APPENDIX: ELEMENTS OF STATISTICS

We assumed that the susceptibility power spectrum is a realization of a stochastic process (see eq. 14). Therefore, the resulting power spectrum for the lithospheric magnetic field $E\{R_l\}$ in eq. (26) is pseudo deterministic and we could in principle derive a probability density function for each degree l that are related to the selected statistical process. The characterization of the statistical process has useful implications for testing the statistical significance of the misfit between the observational and the model SH degree variance.

For example, Hulot & Le Mouel (1994 their section 3) assume that the population $\{g_l^m\}$ have equal variance for each degree l. This

implies (we show it below) that the ratio between the observational R_l and the statistical $E\{R_l\}$ degree variances follows a chi-square distribution X^2_{2l+1} with $2l+1$ degrees of freedom

$$X^2_{2l+1} \stackrel{d}{=} (2l+1)\frac{R_l}{E\{R_l\}}, \tag{A1}$$

where $\stackrel{d}{=}$ means 'equal in the sense of the distribution'. This expression can easily be converted to form the confidence interval of the model SH degree variance

$$(2l+1)\frac{R_l}{X^{2,\max}_{2l+1}(x)} \leq E\{R_l\} \leq (2l+1)\frac{R_l}{X^{2,\min}_{2l+1}(x)}, \tag{A2}$$

where $X^{2,\min}_{2l+1}(x)$ and $X^{2,\max}_{2l+1}(x)$ are such that $X^2_{2l+1}(x)$ has $(100-x)/2$ per cent chance of being less than $X^{2,\min}_{2l+1}(x)$ and an equal chance of being larger than $X^{2,\max}_{2l+1}(x)$.

If we further obtain some evidence that the events $E\{R_l\}$ and $E\{R_{l'}\}$ (with $l \neq l'$) are independent, we could also find the best fit between the observational and the statistical degree variances by maximization of the probability density (for instance Lhuillier *et al.* 2011)

$$pdf(\mathfrak{m}, \varepsilon, \gamma) = \frac{1}{\nu}\prod_l X^2_{2l+1}\left(\frac{R_l}{E\{R_l\}}\right), \tag{A3}$$

where ν is a normalization factor and $\mathfrak{m}, \varepsilon, \gamma$ are, respectively the mean induced magnetization, the mean crustal thickness, and the power law exponent for the spectrum of the susceptibility. These probabilistic considerations are not general but apply to a very specific case. They compel us to examine in more details whether the assumptions made on the susceptibility coefficients and on the power spectrum (see Section 3) are compatible with the statistical framework proposed by Hulot & Le Mouel (1994). The implications are not essential for the present paper but they could be important if we want to better characterize the lithospheric field statistical model rather than focusing on its SH degree variance as was done so far.

A1 Variance of the $\{g_l^m\}$ coefficients

We focused our effort to establish a form for the power spectrum assuming that the susceptibility power spectrum follows a power law (eq. 14). This assumption is not sufficient to define a unique statistical process in space. We thus further assumed that the susceptibility coefficients were uncorrelated (eq. 15).

Let us consider the ratio $\sum_{m=-l}^{l} \frac{(g_l^m)^2}{E\{(g_l^m)^2\}}$, with $E\{(g_l^m)^2\} = \sigma^2_{m,l}$ the variance of the observational Gauss coefficients g_l^m assumed to be independent centred Gaussian variables. This series is a sum of square of independent Gaussian variables of unit variance which, by definition, follows the chi-square distribution of $2l+1$ degrees of freedom

$$X^2_{2l+1} \stackrel{d}{=} \sum_{m=-l}^{l}\frac{\left(g_l^m\right)^2}{\sigma^2_{m,l}}. \tag{A4}$$

Let us then assume that the variance of the $\{g_l^m\}$ is constant over the orders m so that $\sigma^2_{m,l} = \sigma_l^2$ can be taken outside the sum. Then, we can write

$$X^2_{2l+1} \stackrel{d}{=} (2l+1)\frac{\sum_{m=-l}^{l}\left(g_l^m\right)^2}{\sum_{m=-l}^{l}\sigma_l^2}. \tag{A5}$$

Then, multiplying the numerator and the denominator by $(l+1)$ we find

$$X^2_{2l+1} \stackrel{d}{=} (2l+1)\frac{(l+1)\sum_{m=-l}^{l}\left(g_l^m\right)^2}{(l+1)\sum_{m=-l}^{l}\sigma_l^2} = (2l+1)\frac{(l+1)\sum_{m=-l}^{l}\left(g_l^m\right)^2}{(l+1)(2l+1)\sigma_l^2}. \tag{A6}$$

The numerator is by definition the degree variance R_l (eq. 11) of the observed lithospheric field, and the denominator, here $E\{R_l\} = (l+1)(2l+1)\sigma_l^2$, is the degree variance of the stationary isotropic statistical (SIS) model defined by Hulot & Le Mouel 1994 (their eq. 1) so that we retrieve the eq. (A1)

$$X^2_{2l+1} \stackrel{d}{=} \sum_{m=-l}^{l}\frac{\left(g_l^m\right)^2}{\sigma^2_{m,l}} \stackrel{d}{=} (2l+1)\frac{R_l}{E\{R_l\}}. \tag{A7}$$

This demonstrates that the test established by Hulot & Le Mouel (1994) stems from the SIS hypothesis. The great advantage of the SIS hypothesis is that the X^2_{2l+1} statistics is applicable to test the relevance of the ratio between the observational and the expected degree variances (eq. A7) and the relevance of the ratio between the observational and the expected variance of the coefficient g_l^m for each degree l (eq. A4). The equivalence between both distributions no longer holds true if $\sigma^2_{m,l}$ is not equal for all coefficients g_l^m of identical SH degree l.

The statistical model proposed in this paper is a departure from the SIS model. By putting the eq. (15) into the eq. (16), we see that the statistics on lithospheric field coefficients $\{g_l^m\}$ is imposed by the statistics of the susceptibility coefficients $\{\chi_l^m\}$. For a fixed SH degree l, the Gauss coefficients are implicitly assumed to be independent Gaussian centred variables. However, by construction of the induced magnetization (eq. 4), the lithospheric field has a preferred reference frame which is the one aligned in the direction of the Earth's main field axial dipole. An immediate consequence is that the statistical model for the lithospheric field is not isotropic. The set of $\{g_l^m\}$ coefficients have differing variances (eq. 16) by virtue of the two factors α_{l+1}^m (eq. 7) and δ_{l-1}^m (eq. 8) that write

$$\sigma^2_{m,l} = \left(g_1^0 F_l(\varepsilon)\right)^2\left[\left(\alpha_{l+1}^m\right)^2 E\left\{(\chi_{l+1}^m)^2\right\} + \left(\delta_{l-1}^m\right)^2 E\left\{(\chi_{l-1}^m)^2\right\}\right]. \tag{A8}$$

The equivalence in the statistics shown in eq. (A7) would be achieved if we could reasonably assume $\sigma^2_{m,l} \simeq \sigma_l^2$ to set

$$\sum_{l=-m}^{m}\sigma^2_{m,l} \simeq (2l+1)\sigma_l^2. \tag{A9}$$

However, we show that for $m \neq l$

$$\frac{\alpha_{l+1}^m}{\delta_{l-1}^m} \simeq 3, \tag{A10}$$

so that

$$\sigma^2_{l,m} \simeq \left(g_1^0 F_l(\varepsilon)\right)^2 \sigma_\chi^2 (l+1)^{-\gamma}\left(\alpha_{l+1}^m\right)^2. \tag{A11}$$

The maximum of difference within the variances $\sigma^2_{l,m}$ values for a given SH degree l is found between the zonal ($m = 0$) and the sectoral ($l = m$) coefficients and is about

$$\frac{\sigma^2_{0,l}}{\sigma^2_{l,l}} \simeq \frac{(l+1)^2}{2l+1} \simeq \frac{l}{2}. \tag{A12}$$

Therefore, within a set of $\{g^m_l\}$ the variability of the variances cannot be overlooked and the eq. (A9) is not defensible. The *heteroscedasticity* of the population of $\{g^m_l\}$ is in contradiction with the assumptions underpinning the eq. (A1) and therefore the eq. (A2). This is a possible source of bias that makes the chi-square statistics with $2l + 1$ degrees of freedom proposed by Hulot & Le Mouel (1994) not readily applicable in our case for testing the relevance of the statistical lithospheric field degree variance $E\{R_l\}$ by comparison with the observed one R_l.

A straightforward statistical test would be to apply the eq. (A4) with $\sigma^2_{m,l}$ defined by the eq. (A8). However, our aim is not to test the stochastic lithospheric field model that appears in the eq. (10) but, rather, to fit the observed to the statistical SH degree variance. There are many reasons why the statistical and the observational NGDC-720 (Maus 2010) models are not expected to agree coefficient by coefficient. First, our model assumes that the lithospheric magnetic field is induced by an axial main field dipole. This assumption is too simplistic and we cannot neglect the more complex geometry of the main field, particularly in the South Atlantic 'anomalous' region (e.g. Hulot *et al.* 2007). We also cannot exclude the occurrence significant remanent magnetization structures. Secondly, the NGDC-720 Gauss coefficients are by construction smeared with different types of error. For example, the sectoral harmonic coefficients $l \simeq m$ have comparatively larger errors than other coefficients. For the vector satellite data, this is due to correlated errors along the near-polar circular satellite orbits that do not allow recovering accurately the magnetic field components perpendicular to the flight direction (see for instance Kotsiaros & Olsen 2014 for recent simulations). For the aeromagnetic scalar data, this is due to the fact that the transformation of a scalar anomaly grid to a vector magnetic field model is subject to the 'Backus effect' (Backus 1970) that shows a maximum ambiguity on the sectoral Gauss coefficients. These two sources of error, selected for illustration purposes, are in evident contradiction with the stochastic model that predicts comparatively smaller variances for the sectoral coefficients (eq. A12).

A1.1 The dependency of the $\{g^m_l\}$ coefficients

Let us assume that we devised an expression for the statistical distribution for the model degree variance $E\{R_l\}$. Another difficulty arises because the Gauss coefficients $\{g^m_l\}$ for varying degree l and equal orders m are dependent variables. This dependency is immediately apparent by considering the eq. (10) where, by recurrence, the coefficients g^m_l are related to the g^m_{l-2} and the g^m_{l+2} coefficients through the susceptibility coefficient values χ^m_{l-1} and χ^m_{l+1} for a given order m. Let us consider the couple

$$g^m_l = g^0_1 F_l(\varepsilon)\left[\alpha^m_{l+1}\chi^m_{l+1} + \delta^m_{l-1}\chi^m_{l-1}\right], \tag{A13}$$

$$g^m_{l+2} = g^0_1 F_{l+2}(\varepsilon)\left[\alpha^m_{l+3}\chi^m_{l+3} + \delta^m_{l+1}\chi^m_{l+1}\right]. \tag{A14}$$

Reorganizing the equations, we find

$$g^m_{l+2} = \frac{\delta^m_{l+1}}{\alpha^m_{l+1}}\frac{F_{l+2}(\varepsilon)}{F_l(\varepsilon)} g^m_l + g^0_1 F_{l+2}(\varepsilon)\left(\alpha^m_{l+3}\chi^m_{l+3} - \frac{\delta^m_{l-1}\delta^m_{l+1}}{\alpha^m_{l+1}}\chi^m_{l-1}\right). \tag{A15}$$

Since the parameters $\{g^m_l\}$ covary, the probability of occurrence of one coefficient affects the probability of others of identical order and degree parity. In principle, this prevents us to apply the multiplicative rule of probability for independent events if we wished to find a solution to our problem by maximizing a probability density function such as the one described by the eq. (A3). For all these reasons, we failed to solve the inverse problem by using a probabilistic point of view and we relied on a more conservative but well-founded misfit approach such as the one expressed in eq. (28).

A1.2 The covariance matrix of the $\{g^m_l\}$ coefficients

For other applications, like the construction of a covariance matrix for the statistical lithospheric field model, the dependency is not so severe because it involves only the Gauss coefficients of the same order m and the same parity for the SH degree l. We have

$$E\left\{g^m_l g^{m'}_{l'}\right\} = \sigma^2_{m,l}\delta_{mm'},$$

$$E\left\{g^m_{l'} g^m_l\right\} = \left(\upsilon^m_{l',l}\right)^2 \text{ if } \left|l - l'\right| \text{ even and 0 otherwise,}$$

with δ_{ik} the Kronecker symbol. In order to estimate $(\upsilon^m_{l',l})^2$, we first write

$$g^m_{l+2} = \frac{\delta^m_{l+1}}{\alpha^m_{l+1}}\frac{F_{l+2}(\varepsilon)}{F_l(\varepsilon)} g^m_l + \varepsilon_{l+3}, \tag{A16}$$

with

$$\varepsilon_{l+3} = g^0_1 F_{l+2}(\varepsilon)\left(\alpha^m_{l+3}\chi^m_{l+3} - \delta^m_{l+1}\frac{\delta^m_{l-1}}{\alpha^m_{l+1}}\chi^m_{l-1}\right). \tag{A17}$$

and we note that because the susceptibility coefficients are assumed to be centred Gaussian variables then the ε_{l+3} also follows the normal centred law (note as an aside that eq. A16 can be seen as an autoregressive model of order 1). The covariance between g^m_{l+2} and g^m_l simply writes

$$E\left\{g^m_{l+2} g^m_l\right\} = \frac{\delta^m_{l+1}}{\alpha^m_{l+1}}\frac{F_{l+2}(\varepsilon)}{F_l(\varepsilon)} E\left\{\left(g^m_l\right)^2\right\} + E\left\{g^m_l \varepsilon_{l+3}\right\}, \tag{A18}$$

with $E\{(g^m_l)^2\} = \sigma^2_{m,l}$ defined in eq. (A8) and $F_l(\varepsilon)$ in eq. (9). Another level of approximation is needed to make further progress. We use again the ratio (A10) to neglect the terms χ^m_{l-1} in the expressions of the random error ε_{l+3} (eq. A17) and of the Gauss coefficient g^m_l (eq. 10). Noting that by assumption we have $E\{\chi^m_l \chi^{m'}_{l'}\} = \sigma^2_\chi l^{-\gamma}\delta_{ll'}\delta_{mm'}$ (eq. 15) and therefore $E\{g^m_l \varepsilon_{l+3}\} \simeq 0$ so that we get

$$E\left\{g^m_{l+2} g^m_l\right\} \simeq \frac{\delta^m_{l+1}}{\alpha^m_{l+1}}\frac{F_{l+2}(\varepsilon)}{F_l(\varepsilon)} E\left\{\left(g^m_l\right)^2\right\}, \tag{A19}$$

which shows immediately that

$$E\left\{g^m_{l+4} g^m_l\right\} \simeq \frac{\delta^m_{l+3}}{\alpha^m_{l+3}}\frac{\delta^m_{l+1}}{\alpha^m_{l+1}}\frac{F_{l+2}(\varepsilon)}{F_l(\varepsilon)}\frac{F_{l+4}(\varepsilon)}{F_{l+2}(\varepsilon)} E\left\{\left(g^m_l\right)^2\right\}. \tag{A20}$$

Since $F_{l+2}(\varepsilon)/F_l(\varepsilon) < 1$ and using for the last time the estimated value of the ratio (A10), we find that the covariance $E\{g^m_{l'} g^m_l\} = (\upsilon^m_{l',l})^2$ between the Gauss coefficients of identical SH degree parity and order m is significant between two consecutive coefficients ($|l - l'| = 2$) but negligible otherwise. The number of non-zero off-diagonal terms in the SH space covariance matrix is therefore approximately reduced to one for each Gauss coefficient. As a result, the sparsity of the covariance matrix of the lithospheric field stochastic model is numerically very convenient.